SCIENCE CHINA
Chemistry

•REVIEWS•
SPECIAL TOPIC: Rechargeable Battery Technology

January 2024 Vol.67 No.1: 43–66
https://doi.org/10.1007/s11426-022-1525-3

Solid-state lithium-ion batteries for grid energy storage: opportunities and challenges

Xin Chang[1,2†], Yu-Ming Zhao[1†], Boheng Yuan[1], Min Fan[1], Qinghai Meng[1*], Yu-Guo Guo[1,2*] & Li-Jun Wan[1,2]

[1]*CAS Key Laboratory of Molecular Nanostructure and Nanotechnology, CAS Research/Education Center for Excellence in Molecular Sciences, Beijing National Laboratory for Molecular Sciences (BNLMS), Institute of Chemistry, Chinese Academy of Sciences (CAS), Beijing 100190, China;*
[2]*University of Chinese Academy of Sciences, Beijing 100049, China*

Received November 29, 2022; accepted January 31, 2023; published online February 13, 2023

The energy crisis and environmental pollution drive more attention to the development and utilization of renewable energy. Considering the capricious nature of renewable energy resource, it has difficulty supplying electricity directly to consumers stably and efficiently, which calls for energy storage systems to collect energy and release electricity at peak periods. Due to their flexible power and energy, quick response, and high energy conversion efficiency, lithium-ion batteries stand out among multiple energy storage technologies and are rapidly deployed in the grid. Pursuing superior performance and ensuring the safety of energy storage systems, intrinsically safe solid-state electrolytes are expected as an ideal alternative to liquid electrolytes. In this review, we systematically evaluate the priorities and issues of traditional lithium-ion batteries in grid energy storage. Beyond lithium-ion batteries containing liquid electrolytes, solid-state lithium-ion batteries have the potential to play a more significant role in grid energy storage. The challenges of developing solid-state lithium-ion batteries, such as low ionic conductivity of the electrolyte, unstable electrode/electrolyte interface, and complicated fabrication process, are discussed in detail. Additionally, the safety of solid-state lithium-ion batteries is re-examined. Following the obtained insights, inspiring prospects for solid-state lithium-ion batteries in grid energy storage are depicted.

lithium-ion batteries, grid energy storage, solid-state electrolytes, interface stability

Citation: Chang X, Zhao YM, Yuan B, Fan M, Meng Q, Guo YG, Wan LJ. Solid-state lithium-ion batteries for grid energy storage: opportunities and challenges. *Sci China Chem*, 2024, 67: 43–66, https://doi.org/10.1007/s11426-022-1525-3

1 Introduction

Environmental pollution and energy shortage are still the most important concerns of human society [1,2]. Nowadays, the over-reliance on fossil energy has put the world in a plight. On the one hand, the greenhouse gas emissions and the environmental pollution caused by fossil fuel consumption result in an increasingly worsening the loving place for human beings. For example, global climate change has become human development's greatest non-traditional security challenge [3,4]. On the other hand, the increasing energy demands for economic growth conflict with the limited non-renewable resources and the unstable supply chains due to markets and policies [5]. Therefore, developing efficient and economical energy storage systems that serve as a bridge of power supply and consumption is necessary and promising to tackle renewable energy's time and space limitations.

Renewable energy capacity, such as hydropower, solar, wind, bioenergy, accumulates yearly, and the corresponding global weighted average levelized cost of electricity (LCOE) declines [6]. Expanding their share of the existing energy

†These authors contributed equally to this work.
*Corresponding authors (email: ygguo@iccas.ac.cn, qhmeng@iccas.ac.cn)

supply is very favorable. However, the conventional generation and distribution infrastructure require a highly delicate, low error rate and nearly-instantaneous balance between power supply and demand on the grid system. The intermittent nature of renewable energy is a significant constraint to its large-scale deployment in the power system. Therefore, it is necessary that efficient and economical energy storage systems serve as a bridge to connect the different power requirements on the power supply side, the electric power distribution side, and the customer side [7].

The development of energy storage systems is usually application-oriented, and no single energy storage technology can fully meet the demand for large-scale energy storage in the grid. Mechanical energy storage, represented by pumped-hydro storage, is currently the dominant high-capacity energy storage technology due to its long service life and low maintenance costs. However, it has the disadvantages of being influenced by environmental terrain, high initial capital investment, and a long engineering construction cycle. Besides the mechanical-type, chemical-type and thermal-type are also conventional forms of energy storage, while their storage and conversion are limited to widespread use. Electrochemical energy storage, which has the characteristics of pollution-free operation, and high charging and discharging efficiency, has been developing rapidly in recent years [8,9]. Batteries, as the most representative electrochemical energy storage devices, are considered to be more suitable for the large-scale energy storage and can be deployed in homes far from the grid, in cities, and in places inaccessible to traditional electricity infrastructure. The recent progress and challenges of several battery technologies with great application potential in grid energy storage are systematically summarized [10].

In recent decades, the development of lithium-ion batteries (LIBs) has entered a golden period, occupying most of the consumer electronics and powered vehicle markets. LIBs are expected to play a full role in the power system due to their superior performance. For example, they can track and smooth planned powder output, provide auxiliary services, improve the power supply's quality and reliability, adjust the electricity load [11].

Unfortunately, traditional LIBs use flammable organic electrolytes, which are prone to fire and explosion when the batteries undergo thermal runaway [12]. Fire safety challenges for grid-scale LIBs-based energy storage were discussed in detail [13]. Although researchers have done much work on electrode and electrolyte design, the safety hazards of LIBs are still not fully solved. Solid-state electrolytes (SSEs) discard flammable organic solvents to the greatest extent, less prone to thermal runaway and gas production. Furthermore, SSEs with wider electrochemical stability windows and better interfacial compatibility are expected to avoid side reactions as much as possible and prolong cycle life. Besides, solid-state LIBs give more opportunities for extending integration approaches to satisfy the implementary demand of the grid large-scale energy storage.

Solid-state batteries are recognized by academic and industrial circles as the next mainstream direction of battery development, and rapid progress has been made in the past decade. Nickel-rich layered oxide cathodes with the high capacity are considered to be one of the most promising candidate materials for solid-state batteries. Their bulk structure evolution and interfacial reactions during long-term cycling in solid state batteries have been deeply explored [14,15]. Alloy anodes are also worthy of attention as key materials for high energy density solid-state batteries [16]. The NCM811||μ-Si full-cell prepared by Meng *et al*. [17] exhibited excellent cycle life. Furthermore, the safety of solid-state batteries is supported by more experimental evidence and quantitative analysis [18]. These surprising results show us the promise of solid-state LIBs for grid energy storage.

Hence, we summarize the application of conventional LIBs in large-scale energy storage, comprehensively assess their development status and problems, and discuss the opportunities of solid-state LIBs. Although we have high expectations for solid-state LIBs, many problems remain to be addressed. The review comprehensively discusses several solid-state electrolytes and electrodes potentially used in solid-state LIBs for grid energy storage. The interface problems and processing difficulties around these materials are deeply analyzed. Additionally, whether solid-state batteries are safe is assessed from multiple perspectives. After solving the problems of material preparation, interface modification, battery processing, *etc*., the application of solid-state LIBs in grid energy storage is worth waiting.

2 LIBs for grid energy storage

Different energy storage technologies have been developed for large-scale energy storage, which can be divided into the following several types: mechanical (*e.g*., pumped hydro system (PHS), compressed air energy storage (CAES) and flywheels), electrical (*e.g*., capacitor and supercapacitor energy storage (SCES)), chemical (*e.g*., hydrogen storage with fuel), thermal (*e.g*., heat storage using phase-change materials) and electrochemical (*e.g*., lithium-ion, lead–acid, nickel–cadmium, sodium–sulfur, sodium nickel chloride and flow batteries) [19,20]. According to statistics from the China Energy Storage Alliance (CNESA) energy storage project database (Figure 1a), by the end of 2020, the global operational energy storage project capacity is 191.1 GW, an increase of 3.4% in comparison to that in the previous year [21].

The conventional PHS is still the largest energy storage

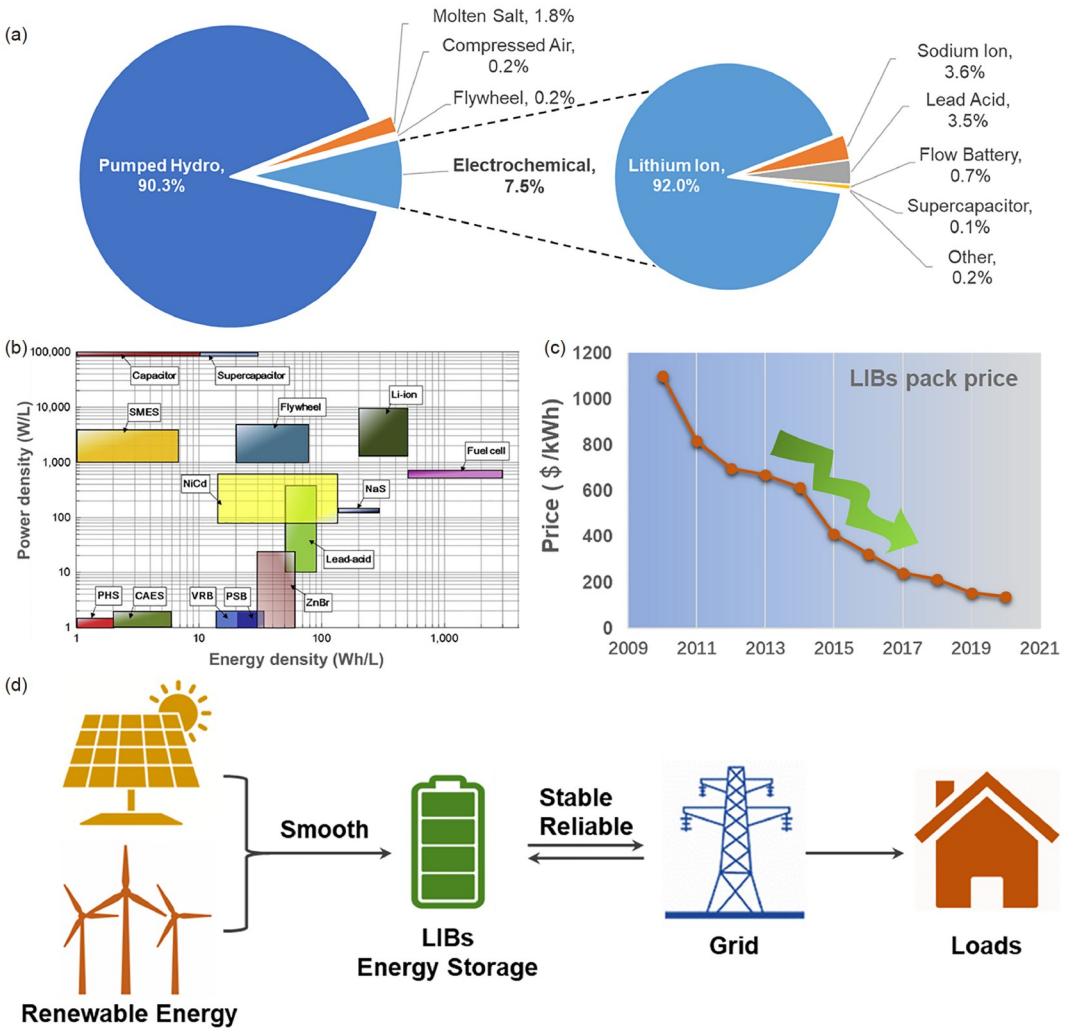

Figure 1 (a) The global operational energy storage market by installed capacity from 2000 to 2020. (b) A comparison of energy and power density of different energy storage systems. Reproduced with permission from Ref. [19]. (c) The annually decreased pack price of LIBs. (d) Integration of renewable energy sources into grid (color online).

capacity contributor, which accounts for 90.3% of all worldwide installed storage capacities. Then, the second largest energy storage contributor is the electrochemical storage system, occupying 7.5% (14.3 GW) of all capacities. Especially, among all the electrochemical storage capacities, LIBs account for 92.0% (13.1 GW), which is undoubtedly the most predominant electrochemical energy storage technique.

2.1 Priorities of LIBs in grid energy storage

LIBs were firstly introduced to the market by Sony Corporation in the 1990s and ever since they were widely used in all kinds of portable electronics and power tools. Currently, after over thirty years of fast growth, LIBs have made significant progress in achieving higher energy density (~250 Wh kg^{-1}), longer calendar (>10 years) or cycle life (>1,000 cycles) [22–24]. Except for the continuing popularity in consumer electronics, they are expected to play a crucial role in dealing with global climate change and creating a sustainable world [22,25]. For example, due to the high energy density and long cycle life, the state-of-the-art LIBs can be applied as a single power source for electric vehicles (EVs) to replace the internal combustion engine in conventional fuel vehicles, so as to reduce the depletion of limited oil resources and carbon dioxide emissions in transportation sectors [26,27]. In the meantime, in order to integrate more renewable energy (such as wind or photovoltaic power) into gird, LIBs have been receiving much more attention and become the most important and fastest growing electrochemical energy storage technique, due to its high round trip efficiency (up to 95%), high energy and power density, low self-discharge rate, no memory effects, rapid response time (in milliseconds), low toxicity, long calendar and cycle life [28].

The reversible intercalation chemistry between the anode (graphite) and cathode (such as lithium nickel cobalt aluminum oxides (NCA), lithium nickel manganese cobalt

(NMC), lithium iron phosphate (LFP), lithium cobalt oxides (LCO) and lithium manganese oxides (LMO)) in LEs endows LIBs excellent stability and high voltage. Even though the organic electrolyte is thermodynamically unstable with electrode materials, a solid electrolyte interphase (SEI) on the graphite anode and cathode electrolyte interphase (CEI) on the cathode would be formed during the first charge–discharge process, which will protect the further reaction between LEs and electrodes during cycling, and ensure the super stable cycling of LIBs [26]. Compared with other electrochemical energy storage techniques (lead–acid, Ni–Cd, Na–S, $NaNiCl_2$ and flow batteries), LIBs exhibit the highest volumetric and gravimetric energy density (Figure 1b). As shown in Table 1, a comparison of different large-scale energy storage technologies is summarized. An outstanding overall performance, including high power and energy density, long duration time, millisecond response time, high round-trip efficiency, low self-discharge, and long lifespan, can be achieved for LIBs, which also explains their dominating role in the electrochemical energy storage market. Currently, MW-grade LIBs-based energy storage stations are operating and installing worldwide, and also are playing an important role in balancing the grid systems (electricity production, transmission, and consumption) and bridging the renewable energy (wind and solar) with grids [20,29].

LIBs are expected to grow rapidly in grid energy storage over the next several years. Except for the overall performance advantages compared with other batteries, relatively high cost is a key challenge for the broader expansion of LIBs in grid energy storage. In fact, the price of LIBs has experienced a great reduction compared to that of ten years ago (*e.g.*, 1,100 \$ kWh^{-1} in 2010 *vs*. 137 \$ kWh^{-1} in 2020) (Figure 1c) [24,30]. In the future, with the growth of market and large-scale production, the average cost of LIBs will undoubtedly continue to decrease [31]. Firstly, a production improvement, by employing advanced manufacturing equipment, the integration of battery packs and streamlining the formation process, will further reduce their cost [32]. Secondly, developing innovative materials, such as cobalt-free cathodes, high specific energy electrode materials (*e.g.*, Si-based anodes, high-capacity and high-voltage cathodes), aqueous binders (eliminating the use of expensive organic solvent during electrode production), will reduce the material or fabrication cost and increase the volumetric and specific energy density of LIBs, so as to contribute to a cost reduction of LIBs in per-kWh [33–39]. Thirdly, improving the performance and making LIBs with longer cycle life will also greatly reduce the life cycle cost of LIBs, even if a relatively higher prior-period investment is probably involved [24,40]. Finally, the reutilization of retired automotive batteries into the gird energy storage and building a closed-loop recycling of spent LIBs will provide additional cost reduction of LIBs [41–43].

2.2 Applications of LIBs in grid energy storage

The applications of energy storage in grid can be categorized by different ways, for example, the power (*e.g.*, frequency and voltage regulation) and energy (*e.g.*, peak shaving, load leveling and energy arbitrage)-related applications, in front of the meter (balancing the transmission and distribution) and behind the meter (load or consumer side), the power rating (small (≤1 MW), medium (10–100 MW) and large scale (≥300 MW)), and the voltage (high, medium, and low voltage grid) [29,44–47]. Due to the flexible power and energy, quick response, high round-trip efficiency characteristics, LIBs are able to satisfy different applications in grid energy storage. Firstly, LIBs-based energy storage systems can provide services to ensure the flexibility, stability, and reliability of grid systems. Secondly, LIBs-based energy storage systems play a crucial role in smoothing the integration of renewable energy into grid systems.

2.2.1 Peak shaving and load leveling

The electric power system transmits and distributes elec-

Table 1 Comparison of different large scale energy storage technologies [44,45,48–52]

Number	Types	Specific energy (Wh kg^{-1})	Volume energy (Wh L^{-1})	Power (W L^{-1})	Efficiency (%)	Discharge time	Response time	Lifetime (year)	Self-discharge (%/day)
1	PHS	0.5–1.5	0.5–1.5	0.5–1.5	65–87	1–24 h+	min	40–60	0–0.02
2	Flywheel	5–100	20–200	1,000–2,000	90–95	ms–min	ms	15+	24–100
3	CAES	30–214	3–6	0.5–2	50–89	1–24 h+	min	20–40	0–1
4	Lead–acid	30–40	50–90	10–400	70–90	s–h	ms	3–15	0.033–1.10
5	Ni–Cd	50–75	60–150	150–300	60–90	s–h	ms	10–20	0.07–0.71
6	Na–S	150–240	150–250	150–230	80–90	s–h	ms	10–15	20
7	$NaNiCl_2$	90–120	150–180	220–300	85–90	s–h	ms	10–14	11.89–26.25
8	LIBs	100–265	200–700	500–2,000	90–97	min–h	ms	5–20	0.03–0.33
9	Flow battery	25–85	16–90	40–100	60–85	12 h	ms	5–15	Small
10	SCES	<10	2.5–15	500–5,000	85–98	ms–h	ms	20+	0.46–40

tricity from power plants to consumers in one-way method, which means that the power generation should always match the load. However, the demand for electricity varies momentarily, daily, and seasonally, and the maximum demand may last for only a short period of time. In this case, building power generation to meet the peak loads or adjusting the generation capacity frequently to match the loads would be inefficient and expensive. Therefore, a peak shaving and load leveling function is highly necessary to the grids [47]. Peak shaving serves to store energy in low-demand periods and release energy to the grid at peak periods, so as to shift the peak demand to the off-peak periods. Load leveling tries to flatten the entire load curve, which reduces the power demand during high-demand periods by discharging and storing energy immediately during low-demand periods by charging. Peak shaving and load leveling require that the energy storage technology must be able to store and release a large quantity of energy for some minutes to some hours. Due to the high power and energy density, and high round-trip efficiency, LIBs exhibited promising potential for peak shaving and load leveling applications [19,47].

2.2.2 Voltage and frequency regulation

The electric power system needs to control its voltage and frequency within a standard limit so as to maintain the stability and reliability of grid. The flow of reactive power and the existing of transients and harmonics in the grid systems will lead to a voltage fluctuation [19,47]. The mismatching of power consumption and generation within a grid will lead to the slow down or speed up of generators, and therefore the decrease or increase of grid frequency [47]. Especially, due to the intermittent and fluctuating feature, the integration of renewable energy will cause increasingly serious voltage and frequency fluctuation. The imbedding of energy storage systems with local real power–frequency and reactive power–voltage droop controllers could enhance the voltage and frequency stability effectively [53]. Correspondingly, it requires the energy storage system with a quick response, high rate and power performance, which could be well satisfied by the LIBs-based energy storage technique [54]. Characterized by high power and energy density, long duration time, millisecond response time, high round-trip efficiency, low self-discharge, long lifespan, pollution-free operation and low maintenance, LIBs represent one of the most attractive electrochemistry energy storage technologies for the grid storage applications.

2.2.3 Integration of renewable energy

Renewable energy sources, such as wind and solar energy, are widely and abundantly distributed on earth. Making full use of these renewable energy sources will largely reduce the depletion of nonrenewable fossil-based energy, so as to contribute to a sustainable world. Especially, integrating more renewable energy sources into grid systems is becoming a global consensus. Over the past few decades, the share of installed capacity by wind and photovoltaic power has been increasing continuously, and unquestionably, the growth will be accelerated in the future [49,55]. One problem is that the renewable energy sources are usually intermittent and fluctuating. Directly integrating renewable energy sources into a grid will cause unacceptable disturbance or even failure to the grid. Therefore, an energy storage system that functions to ensure the energy quality and security by renewable energy sources is inevitable. Besides, the unpredictability of renewable energy sources (especially for the wind power) will result in frequently mismatch between power generation and demand. In this case, the energy storage system storing excess energy from renewable sources and releasing them in the peak demand is quite necessary. In short, the energy storage system serves to make better use of the renewable energy sources and ensure their smooth integration into the grid systems (Figure 1d) [49,56,57]. LIBs could offer high specific power/energy density, high round-trip efficiency and longer cycle life, and is becoming more and more popular for utilizing renewable energy sources. A fast-growing LIBs' market that aims to promote the increased penetration of renewable energy into the grid is highly expected in the coming years. For example an increase from 2 GWh per year in 2020 to 30 GWh per year in 2030 has been estimated [49,58,59].

2.3 Degradation and safety issues of LIBs in the grid energy storage

At present, most of the LIBs used for energy storage are composed of an anode, a cathode, a plastic separator, and a liquid non-aqueous electrolyte. Reversible Li^+ intercalation and deintercalation occurred between the anode and cathode during charging and discharging. The Li^+-intercalated graphite anode or deintercalated cathode is thermodynamically unstable to the liquid non-aqueous electrolyte. A passivated SEI and CEI would be formed at the electrode/electrolyte interfaces during charging and discharging, providing the dynamic stability of LIBs. Nowadays, under the deep cycling, the state-of-the-art LIBs can maintain thousands of cycles, and no maintenance is required. However, an aging or degradation process, caused by the complex side interactions of all cell components, will inevitably happen after LIBs have been activated [60]. LIBs represent one of the most promising and fastest growing electrochemical energy storage technologies. Studying and understanding the aging or degradation process of LIBs is significantly important for enhancing their performance and safety.

2.3.1 Degradation of LIBs for grid energy storage

The degradation of LIBs is caused by a series of complex

side reactions, which involves all the components in the cell, including electrodes, electrolytes, separators, and current collectors. The degradation of LIBs can be divided into mainly two parts: during the storage (at rest) and during the operation (cycling) [61–63]. The aging process during the storage may lead to self-discharge, capacity loss, potential change, increased impedance, and thus affect the calendar life of LIBs. During the initial charging, lithiated graphite and delithiated cathodes are formed, which are thermodynamically reactive to the organic solvents (*e.g.*, ethylene carbonate (EC), diethyl carbonate (DEC), dimethyl carbonate (DMC), ethyl methyl carbonate (EMC), and propylene carbonate (PC)) and Li salts (mainly, lithium hexafluorophosphate ($LiPF_6$)) in liquid electrolytes. A complicated redox reaction will happen at the electrode/electrolyte interfaces to form a passivated SEI layer on the graphite anode and CEI layer on the cathode, accompanied with the gas release and consumption of active Li (Figure 2) [61]. The SEI or CEI layer, to some extent, prevents the further reaction between the electrolyte and charged anode or discharged cathode, and ensures the dynamically stable cycling of LIBs.

However, during the storage, the SEI will continue to grow with time and consume active Li, thereby leading to increased impedance and capacity loss. Meanwhile, a positive potential shift would be caused by the continuous loss of active Li, promoting the overcharge and degradation of cathodes. As for the cathode, a growth of CEI by oxidizing electrolytes, and a phase change and dissolution of transition metal of cathodes will happen continuously, resulting in reduced charge capacity and increased resistance. The aging of LIBs at rest is also related to their storage temperature and the state of charge (SOC). Higher temperature and higher SOC will lead to an accelerated aging of LIBs [61,64]. Except for the aging on the anode and cathode, other electrode components, like conducting agents, binders, current collectors, separators and electrolytes, may become deteriorated with time and lead to the degradation of LIBs [63].

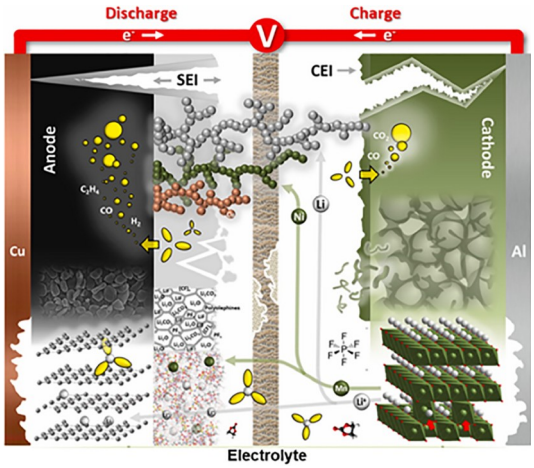

Figure 2 Schematic degradation mechanisms of LIBs. Reproduced with permission from Ref. [61] (color online).

The degradation of LIBs during the operation is related to much more factors, including the depth of discharge (DOD), rate, structure evolution, overcharge, heat generated during the charging and discharge, SEI or CEI breaking and rebuilding, mechanical degradation, Li metal plating. As shown in Figure 2, Li metal plating may occur on the graphite anode during over-charging, fast charging, or charging at low temperature, which is extremely detrimental to LIBs [65]. During repeated charging/discharging cycling, volume changes by phase transformation of cathode materials will lead to particle cracking, mechanical disintegration, and contact loss with conductive carbon or current collectors [66–68].

In practical applications, LIBs for grid energy storage are assembled by more than thousand cells in parallel or in series in order to achieve a specified current and voltage capability, which also makes the operation of each cell under quite similar conditions extremely challenging [69]. In this case, when LIBs were fully charged, some of the cells may be overcharged. Overcharging of cathodes often occurs when the active Li content is low within a cell, leading to irreversible phase transformation, lattice imperfection, accelerated side reactions, and poor thermal stability of cathode materials [60,70,71]. Due to lower cost and very stable lattice structure, the olivine-structured LFP cathode shows much more advantages than other cathode materials (*e.g.*, NCA, NCM, LMO), making it the most popular and the fastest-growing LIBs' type for grid energy storage applications in the future [62,72]. In addition, the generated ohmic heat during the charging and discharging can also aggravate the side reactions within cells, and thus accelerate the degradation of LIBs. The degradation and the aging of LIBs involve a series of complicated physical and chemical reactions within the cells, and are related to all aspects of batteries including fabrication, operation, and storage. Understanding the degradation mechanism of LIBs is essential for developing realistic models for lifetime prediction and battery diagnosis, exploring novel strategies to further enhance the performance and safety of battery, and thus making LIBs a more powerful tool for grid energy storage.

2.3.2 Safety issues of LIBs for gird energy storage

LIBs are a promising technology for the grid energy storage application and the globally installed capacity by LIBs has experienced a rapid growth in the past few years. However, the frequently occurring fire or explosion incidents involving LIBs-based energy storage stations have posed serious threat to the public safety and caused great concerns to this technology [73]. For example, more than 20 energy storage-related fire incidents have been reported in South Korea between August 2017 and December 2018, which led to significant stagnation of local energy storage industry

[73,74]. According to the investigations, many faults, including the failure of the protection systems during the battery operation, fluctuated ambient temperature, lack of an overall control and protective system, could be summarized as the causes that triggered the thermal runaway of LIBs.

Usually, LIBs are safe when they are stored and operated at manufacturer-recommended nominal conditions [75]. LIBs are fragile and prone to thermal runaway, fire, or even explosion under the off-nominal conditions, such as overcharge, over-discharge, short circuit, overheat, mechanical crash, vibration, shock [76–78]. The recommended maximum operating temperature for LIBs is around 45 °C. Due to some internal or external causes, the temperature of LIBs starts to rise. Once the temperature exceeds the normal operating range, side reactions within the cell will be accelerated and some exothermic reactions tend to occur, which makes the battery unstable with high risk of thermal runaway. As shown in Figure 3, when battery temperature rises to ~69 °C, the SEI on the graphite anode starts to decompose, leading to the exposure of lithiated anode to electrolyte [12]. The exposed lithiated anode will react with liquid electrolyte to release flammable hydrocarbon gases (*e.g.*, methane, ethane) accompanied with heat generation. When the battery temperature is above ~130 °C, the polyethylene (PE)/polypropylene (PP) separator begins to melt and shrink, so that an internal short-circuit occurs and the battery becomes deteriorated rapidly. At a temperature of ~200°C, the layered metal oxide cathode starts to decompose and release oxygen [79]. In the end, the sharply accumulated chemical energy will be released in the form of fire or explosion in most cases [12,77,78]. More seriously, the thermal runaway in a single cell will initiate thermal runaway in adjacent cells, and finally result in the disastrous consequences of the entire battery system [78].

Among all the components that make up a cell, the liquid electrolyte (consisting of flammable organic solvents and thermally unstable lithium salts) and plastic separator (PP/PE) are recognized as the most flammable and fragile parts during thermal runaway. The severe volatility and decomposition of electrolyte could be initiated at a lower temperature range (130 °C–200 °C), and produce a lot of flammable gases. It is reported that the electrolyte combustion can release an energy several times larger than the electrical energy stored in a battery [80]. The porous separator plays a crucial role in preventing the physical contact between the cathode and anode, and providing the Li^+-transporting channels between them [77]. However, the commonly employed PP and PE separators will suffer from severe shrinkages at a temperature above 130 °C, so that an internal short circuit and rapidly accelerated thermal runaway will happen in the LIBs. As a result, developing safe electrolyte and separators, which can mitigate the thermal runaway of LIBs under abusing conditions, is significant to enhance the safety and eliminate the safety concerns on LIBs [12,77,78].

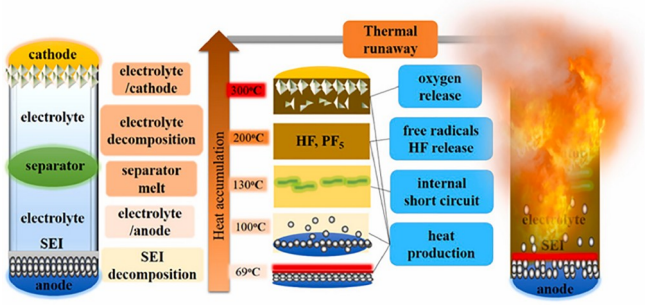

Figure 3 The schematic thermal runaway process of LIBs. Reproduced with permission from Ref. [12] (color online).

3 Opportunities of solid-state LIBs in grid energy storage

3.1 Superiority of solid-state LIBs in grid energy storage

As the representative technologies of energy storage, rechargeable batteries, especially LIBs, play a key role in the decarbonization. Due to the great advantages of a short construction period, low investment, no geographical restriction, strong electricity regulated ability and high energy efficiency, the global LIBs' market has been moving into the surge mode judging from the figures reported in recent years. Given the economic and sustainable development of LIBs, it is important to take the revolution of high safety, low cost, and facile recycle into consideration for large scale energy storage based on LIBs [26]. However, as described above, conventional LIBs apply flammable liquid electrolyte in the system, which very likely results in the primary thermal runaway risks [81,82]. Besides, complicated side reactions accompanied with the charging and discharging process usually reduce the electrochemical performance of batteries [83,84]. However, safety and cycling stability issues are extremely important especially for MW- and even GW-grade energy storage concerning the huge amounts of energy containing inside the system. On the other hand, the cost of the rechargeable LIBs has fallen dramatically over decades benefiting from the rapid growth of processing technologies. However, in view of the large scale of energy-storage system, service life and cost of maintenance, great efforts still need to be made for reducing the cost of batteries, and much attention should be paid for ensuring the green and sustainable development of LIBs, simultaneously. Effective strategies for averting a looming e-waste crisis are designing batteries for easier recycling, which will create pathways for battery manufacturers to build sustainable production-to-recycling full lifecycle processes and reduce the likelihood of a battery waste crisis in the coming decade [85].

Solid-state LIBs employ ionically conductive SSEs (oxide-based, sulfide-based ceramics, solid polymers, or their composites) as opposed to the LEs used in conventional LIBs [86,87]. Active material, SSEs, and conductive carbon are mixed to obtain ion- and electron-conductive electrode composite. Solid-state LIBs are prepared by stacking cathode composite, SSEs, and anode composite layer by layer. In principle, the basic mechanism for energy storage is not changed. During the process of charging, Li^+ are extracted from the cathode and migrate to the anode *via* the solid electrolyte, while electrons transfer from the cathode to the anode through external circuit. In this process, oxidation and reduction reactions take place at the cathode and anode sides, respectively [88]. However, solid-state LIBs show prominent strength over conventional LIBs for applying in grid energy storage.

3.1.1 *Enhance the safety of energy storage batteries*

It is expected that making the solid electrolyte enables lesser safety issues than LE-based conventional LIBs [89]. Usually, the easy growth of Li dendrites during the charging process resulted from inhomogeneous structure of electrodes, disproportion of the ion concentration, overcharge, and polarization, leading to the battery short-circuit and poor safety problems [90]. Besides, the risk of solvent flammability at elevated temperatures is especially apparent when the battery encounters accidently abuse or damage by unpredicted impact or crush.

SSEs usually have a high shear modulus which is considered to suppress the dendrite growth and to prevent short-circuit [88]. The characteristics of no corrosion, no volatilization, no leakage for the SSEs reduce the probability of battery combustion, and abrupt temperature rise resulting from internal short-circuit. Especially for solid-state LIBs, thermally stable electrodes and SSEs, and moderate energy density are beneficial to improve the safety compared with conventional LIBs or lithium-based high energy batteries [91,92]. Besides, thermal stability of some SSEs allows the battery to operate at relatively high temperatures which is fatal for LE-based conventional LIBs as the lithium salt like $LiPF_6$ decomposes above 55 °C [93]. In general, the intrinsic safety features of SSE strategy for LIBs will lead to the development tendency and realize the iteration of grid energy storage quickly [94].

3.1.2 *Extend integration approaches*

Considering the demand for outputting high energy and power, conventional LIBs are usually integrated in grid energy storage systems. Voltage and total energy will be extended by connecting the batteries in series [95]. Similarly, the capacity and total energy will be extended by connecting the battery in parallel. In fact, series and parallel connections are both applied in energy storage systems for improving the voltage, capacity, and total energy at the same time. As for conventional LIBs, the series connections are realized only outside the batteries (in-series connection will have the short-circuit problem, see Figure 4a). As shown in Figure 4b, bipolar stacked solid-state LIBs can be fabricated by layering two or more single-layer batteries without short-circuit due to the introduction of solid electrolytes. In this way, solid-state LIBs can highly enhance the capability of cell design by carrying out the in-series stacking and bipolar structures within a single package. The reduction of the unused room between single cells for conventional LIBs equals the increase of mass and volume energy density. Besides, the parallel stack structure is also available for solid-state LIBs to improve the capacity like conventional LIBs (see Figure 4c) [96]. Besides, liquid-free environment in solid-state LIBs provides the convenience of implanting functional sensors in the cells for *operando* monitoring the data of temperature, resistance, voltage and current, *etc*. [97,98]. In summary, solid-state LIBs give more opportunities for extending integration approaches to satisfy the complementary demand of grid large scale energy storage.

3.1.3 *Improve the performance of batteries*

The substitution of LEs into SSEs introduces enormous advantages on the performance for the battery system. Usually, the dissolution of transition-metal elements, such as Mn, Co, Ni and Fe from the cathode to the liquid electrolyte and their subsequent deposition on the anode, results in ongoing liquid electrolyte reduction, electrode–electrolyte interface and impedance growth as well as the significant capacity degradation upon cycling [99]. Besides, LEs show higher

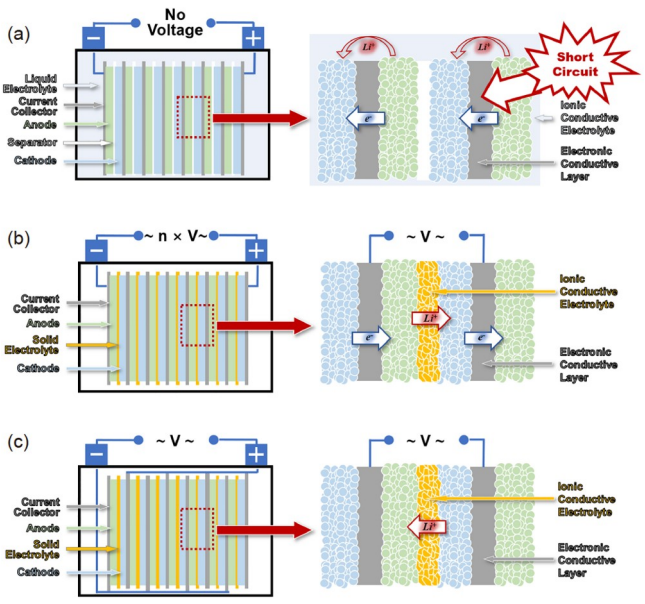

Figure 4 The schematic of internal connections for LIBs. (a) In-series stacking of conventional LIBs. (b) In-series stacking of solid-state LIBs. (c) Parallel stacking of solid-state LIBs (color online).

chemical reactivities than SSEs when they come to the charging and discharging process in LIBs, and the constant side reaction between LEs and electrodes also leads to the capacity degradation similarly [100]. The high reliabilities of solid-state LIBs are derived from both the wide electrochemical window of SSEs, and no solvation–desolvation process between the electrode and electrolyte interface [101]. Besides, SSEs also show low chemical reactivity with electrodes and coatings, impeding the shuttle effect of transition-metal elements. Furthermore, the sensibility of the introduction of impurities during the manufacturing of LIBs will be reduced, and some novel processing technology like dry electrode manufacturing and prelithiation solution can be easily integrated with the practical processing route [102,103]. In this way, the productivity efficiency increases and cost reduction realizes simultaneously. According to the aforementioned analysis, excellent cycling performance with no capacity loss over ten thousand of cycles is expected to be realized in solid-state LIBs [104]. Cost per kilowatt hour of energy storage will be reduced owing to the extension of solid-state LIBs' lifetime. This is another promising advantage solid-state batteries claiming to offer in the large-scale energy storage application scenarios.

3.1.4 Improve the recyclability of LIBs

As discussed before, the recycle of LIBs is a burning issue especially at this era in which the market of grid scale energy storage grows exponentially. However, conventional LIBs we used are highly complicated and sophisticated in structure with the consideration of safety, and not designed for the recyclability at the end of life [105]. Greater efforts must be made to conduct the recyclable design for solid-state LIBs. Besides, novel green recycling technologies, such as cascade utilization, green dissolution, transition-metal element-based selective extraction and biological recovery, are in the urgent stage to be developed [106–109]. As solid-state LIBs are still developing, there is a significant opportunity and time to design and develop recycling processes with the guidance of sustainable principles. In fact, the recycling of solid-state LIBs is intrinsically safer than that of conventional LE-based LIBs without using flammable components [110]. This feature dramatically reduces the complexity and cost of recycling, and processing like crush can be safely realized for solid-state LIBs even with stored energy inside [111].

3.2 Application of solid-state LIBs in grid energy storage

The solid-state LIBs are thought to be a major competitor to conventional LIBs and show a promising strategy to satisfy the requirements for grid scale energy storage in a safer way, as the liquid electrolyte is replaced by a solid-state counterpart. However, we must acknowledge that it will be years to realize the industrialization of solid-state LIBs even though scientists and engineers worldwide show great interest on them [112]. The research and the development of solid-state LIBs (focus primarily on lithium metal-based solid-state batteries for electric vehicles) are mainly concentrated in five countries and regions: the United States, Europe, Japan, South Korea, and China. In the United States, both governments and companies have invested heavily in the research and innovation of solid-state batteries. As the key materials in solid-state batteries, novel SSEs (such as oxide-, sulfide-, halide-based ceramics or glasses) and their composites are intensively investigated. For example, the U.S. Department of Energy (DOE) funds a number of solid electrolyte-based laboratory projects to advance the development of lithium batteries [113], and some emerging innovative companies like Solid Power [114], Solid Energy Systems [115], Ionic Materials and Quantum Scape [116] have accumulated distinctive advantages on organic and inorganic solid electrolytes. The Europe also approves abundant funding to support the development of highly innovative and sustainable technologies for LIBs (liquid and solid-state electrolytes) that last longer, have shorter charging times, and are safer and more environmentally friendly than those currently available [117]. Japan and South Korea starts the industrial layout of solid-state batteries in an early stage, with the highlight of sulfide-based solid electrolytes. Some challenges still need to be conquered in sulfide-based electrolytes even though great breakthrough has been made by companies like LG Chem [118], Samsung SDI [119], Toyota Motor Corporation [120]. Despite a late start, China takes much motivational action for the promotion of the development of solid-state batteries in the field of electric vehicles and scale energy storage according to the outline of the 13th, 14th Five-Year Plan and the Long-range objectives through the year 2035 [121,122]. Over the past two decades, China has come to dominate the conventional liquid electrolyte-based LIBs' market from end to end. As the performance reaching the fundamental limitations, industry leaders, such as Contemporary Amperex Technology Co. Limited (CATL) [123], Ganfeng Lithium Group [124], and Prologium [125], are proceeding rapidly on the research and industrialization of solid-state batteries.

According to statistics, more than 600 lithium-ion battery energy storage systems with different scales have been widely deployed around the world [126]. Representative projects such as Hornsdale Power Reserve [127], Clinton County BESS [128], and Germany Residential Energy Storage Systems [129], have been put into operation. In the pursuit of safer and superior performance, solid-state LIBs are considered to be a better choice for energy storage systems. Zendure, as the first company to announce the application of semi-solid-state battery technology in home energy storage system, released SuperBase V series of products with

a single module capacity of 6.438 kWh, which can break a maximum capacity of 64 kWh [130]. Furthermore, advanced solid-state batteries have been used in grid-scale energy storage projects. China Electric Power Research Institute applied solid-state LIBs to a 1 MWh energy storage container demonstration project [131]. Shandong Power Grid started construction of a 300 MW/600 MWh energy storage demonstration project in August 2022, which would adopt lithium-ion batteries, sodium-ion batteries and solid-state batteries to work together [132]. In summary, the facing challenges now are only temporary, and both academia and industry are fully confident in the development prospects of solid-state LIBs.

4 Challenges of solid-state LIBs in grid energy storage

Although numerous studies are devoted to developing solid-state LIBs, there is still a gap compared to conventional LIBs. The key to improving the performance of solid-state LIBs lies in preparing SSEs with high ionic conductivity. The main directions of current research are solid polymer electrolytes, solid inorganic electrolytes, and composite electrolytes. We know that none of them may perfectly replace the existing liquid systems. The reasons behind it are the mist shrouding the electrode/electrolyte interfaces and the many challenges in processing SE. Especially preparing large-capacity cells with inorganic electrolytes and reducing the manufacturing cost of solid-state batteries are crucial for scale applications.

Up to now, the research on solid-state batteries has mainly focused on lithium metal batteries with high energy density instead of LIBs. Low-cost, long-life, and high-safety battery systems for grid energy storage lack a systematic summary. This chapter will systematically review solid-state lithium-ion battery key materials and advanced technologies suitable for large-scale energy storage. Combined with the thermal runaway mechanism of LIBs, the safety of solid-state LIBs is comprehensively evaluated.

4.1 Key material design for solid-state LIBs

4.1.1 Electrolyte design

Various SSEs have been recently investigated, including solid polymer electrolytes (SPEs) and solid inorganic electrolytes and their composites. Solid inorganic electrolytes can be roughly categorized into oxide- and sulfide-based electrolytes. The characteristics of each solid electrolyte are summarized in this section.

Solid polymer electrolytes. Since Wright's report on the conductivity of the mixture of alkali metal ions and poly (ethylene oxide) (PEO) [133], Armand further expanded the PEO as a solid electrolyte for LIBs, which set off a wave of research on SPEs [134]. The main problems of solid polymer batteries are that they can only operate at high temperatures due to low ionic conductivity and are not resistant to oxidation. In recent decades, extensive research has been carried out around monomers synthesis, structural design, polymerization methods, and preparation of composite materials, aiming to address both challenges.

The Li^+ transport in PEO originates from the high donor number for Li^+ of EO units and the intense mobility of the PEO segment. Thus, the most direct approach is the screening and design of easily dissociated lithium salts. Compared with traditional inorganic lithium salts, more designable organic lithium salts have the advantages of high ionic conductivity, wide electrochemical stability windows, and good thermal stability. Zhang *et al*. [135] systematically explored the effects of LiTFSI, LiFSI, and CF_3SO_3Li on battery performance. The SPE with LiTFSI has a higher ionic conductivity and discharge specific capacity, which benefited from the low crystallinity and the high Li^+ transference number. Meanwhile, the existence of LiFSI is conducive to generating smoother and denser SEI.

Regulating macromolecular structures is a unique approach to improving ionic conductivity [136]. Crosslinking is the most common method of polymer modification, which imposes restrictions on the chains' motions to assume the correct position for crystallization. Duan *et al*. [137] constructed an *in-situ* plasticized PEO-based electrolyte with a double network by regulating the chain length of two oligomers. The prepared SPE exhibits enhanced ion conductivity (5.4×10^{-5} S cm^{-1}), a wide electrochemical window (4.7 V *vs*. Li^+/Li), and impressive mechanical flexibility. In addition to chemical crosslinks that form covalent bonds between molecules, the interpenetrating polymer network (IPN) is a novel type of polymer blend composed of crosslinked and linear polymers. The IPN morphology could also reduce the existence of crystalline domains to nearly disappear. Homann's work [138] proves that IPN improves ionic conductivity, enhances mechanical stability, and broadens the electrochemical window.

Hyperbranched polymers are highly branched macromolecules with three-dimensional dendritic architecture [139,140], so they are entirely amorphous and have many free chain ends, which is propitious to Li^+ transport. Chen *et al*. [141] prepared a polymer electrolyte with hyperbranched PEO as the core and linear PS as the arms. As shown in Figure 5a, the intermolecular entanglement of PS fragments constructed rigid domains, which did not limit the activity of the flexible PEO segment. The hyperbranched structure design is crucial for balancing the enhanced conductivity and mechanical properties.

Some advanced synthesis methods and novel design concepts have brought new brilliance to PEO electrolytes in

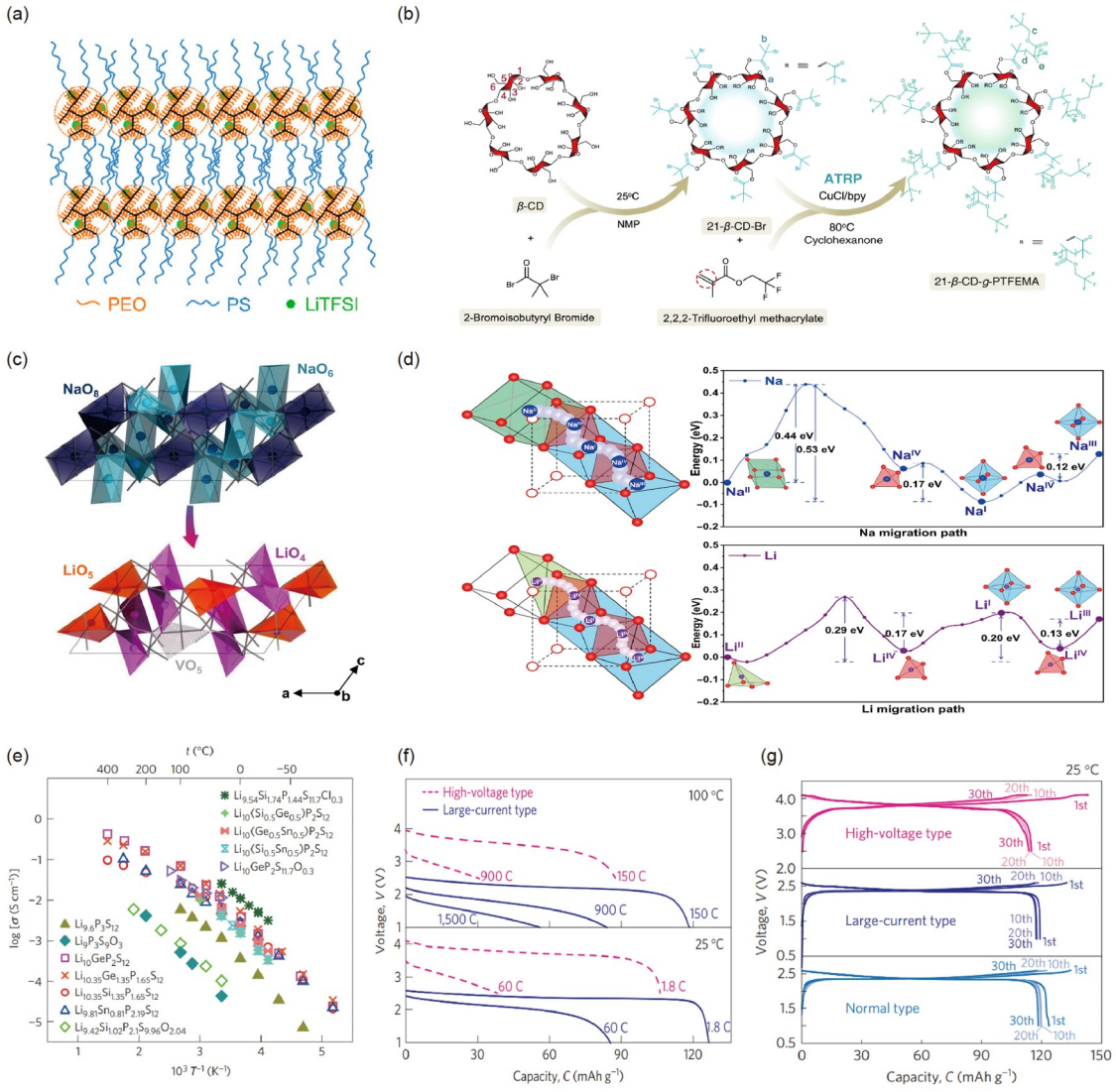

Figure 5 Solid electrolytes design. (a) Illustration of hyperstar polymers topology. Reproduced with permission from Ref. [141]. (b) Schematic of the interactions in the composite electrolyte. Reproduced with permission from Ref. [142]. (c) Skeleton-retained cationic exchange approach to producing $Li_3Zr_2Si_2PO_{12}$. (d) Single-ion migration mechanisms of Na^+ ions and Li^+ ions from solid electrolytes. Reproduced with permission from Ref. [152]. (e) Ionic conductivity of the LGPS family and $Li_{9.6}P_3S_{12}$ and $Li_{9.54}Si_{1.74}P_{1.44}S_{11.7}Cl_{0.3}$. (f) Discharge behavior of the sulfide-based all-solid-state cell with different current densities. (g) Charge-discharge curves of the sulfide-based all-solid-state at 0.1 C. Reproduced with permission from Ref. [163] (color online).

recent years. Zhang *et al*. [142] proposed a top-down design concept and synthesized PEO-based electrolyte with multi-arm topological structures. Due to the introduction of supramolecular interactions and multi-arm topological structures, the comprehensive properties such as high voltage stability, mechanical strength, thermal stability, ionic conductivity, and Li^+ transference number were improved. Multiple Li^+ coordination sites and complex hydrogen-bonding networks worked together for superior ion transport properties (Figure 5b). The resulting improvement for electrochemical performance was confirmed in various full alkali metal cell configurations. Numerous articles have demonstrated the effectiveness of structure design for improving ionic conductivity, while further theoretical guidance is still lacking.

Besides PEO-based SPEs, tremendous solid polymer electrolytes including polyacrylonitrile (PAN), polycarbonate (PC), polymethyl methacrylate (PMMA), polyvinylidene fluoride (PVDF), and poly(vinylidene fluoride-hexafluoropropylene) (PVDF-HFP) have been attracting wide research attention [143]. These materials overcome the shortcomings of PEO-based electrolytes to a certain extent [144].

The introduction of strong polar groups into the polymer molecular structure is beneficial to improving its ionic conductivity. For example, poly(vinylene carbonate) (PVC), polyethylene carbonate (PEC), and polypropylene carbonate (PPC) have attracted widespread attention [145]. Chai *et al*.

[146] prepared a novel kind of PVC/lithium difluoro(oxalato) borate (LiDFOB)-integrated SPE *via in-situ* thermally initiated polymerization, providing improved interfacial compatibility with the electrodes. The traditional PEO electrolyte has poor oxidation resistance, and its decomposition at the cathode interface is one of the reasons for the failure of polymer-based batteries. According to theoretical calculation, the HOMO of PAN and PVDF was lower than that of PEO, which means that the former has better compatibility with high-voltage cathodes [147]. Therefore, many researchers aimed at PAN- or PVDF-modified composite solid electrolytes with wide electrochemical windows, which will be discussed later.

Considering environmental and climate changes, batteries for grid energy storage need to maintain normal operation under wide temperature range. The decline in the ion transport performance of solid-state electrolytes at low temperatures is a fatal blow to batteries. Li *et al*. [148] designed a homogeneous solid-state polymer electrolyte which enabled a $LiFePO_4$ cathode to achieve a superior cycling life and remain 82% of room-temperature capacity at 0 °C. Besides the low ionic conductivity of solid electrolytes, poor interface contacts greatly limited the long-term operation stability of batteries at low temperatures. A quasi-solid polymer electrolyte was fabricated by *in-situ* ring-opening polymerization of 1,3-dioxlane with fluoroethylene carbonate as the plasticizer, giving it a remarkable ionic conductivity and Li^+ transference number (2.4×10^{-5} S cm^{-1} at −60 °C and 0.55 at −20 °C) [149].

Inorganic solid-state electrolytes. Inorganic solid electrolytes are a class of super ion conductor materials. Their bulk ionic conductivity greater than 1 or even 10 mS cm^{-1} has been achieved at room temperature. However, the oxide-type SSEs' growth has been limited by high resistance at grain boundaries. The ubiquitous brittleness of ceramic materials also complicates the processing of oxide-based SSEs. Sulfide-based solid-state electrolytes exhibit high conductivity *via* cold pressing, so there have been a few examples of large-capacity cell preparation in all-solid-state batteries. However, sulfide is very sensitive to water, which requires strict control of low humidity during the production. It is worth noting that although S is abundant and cheap, battery-grade Li_2S as a precursor used in sulfide-based electrolytes is too expensive for large-scale preparation. Hence, many technical challenges still need to be improved through material design. The following paragraphs will discuss the performance and recent progress around oxide-type SSEs, such as NASICON-type and garnet-type, and sulfide-type SSEs, including crystalline and amorphous materials.

The ion conductivity of NASICON materials is limited by the bulk phase and grain boundary resistance. Researchers have worked hard on these two aspects to improve their conductivity. Presently, the prevailing NASICON-type SSEs are derived from Al-doped $Li_{1+x}Al_xTi_{2-x}(PO_4)_3$ (LATP) and $Li_{1+x}Al_xGe_{2-x}(PO_4)_3$ (LAGP) systems. $Li_{1.3}Al_{0.3}Ti_{1.7}(PO_4)_3$ electrolyte prepared by Aono *et al*. [150] has an ionic conductivity as high as 7×10^{-4} S cm^{-1}. The mechanisms behind the Li-ion conductivity enhancement are attributed to the increase of the sintered pellet density and the formation of less-resistive grain boundaries. In addition, the substitution of Al increases the number of charge carriers to balance the valance. Similar effects caused by trivalent cation doping are also observed in the LAGP phase [151].

Recently, Tang *et al*. [152] proposed a skeleton-retained cationic exchange approach to preparing a novel solid electrolyte of $Li_3Zr_2Si_2PO_{12}$(LZSP) originating from the NASICON-type ionic conductor of $Na_3Zr_2Si_2PO_{12}$ (NZSP) (Figure 5c). The calculated migration paths with corresponding relative energies of NZSP and LZSP are shown in Figure 5d. It achieves low activation energy of 0.21 eV and the highest ionic conductivity of 3.59×10^{-3} S cm^{-1} among oxide-type SSEs at room temperature. LZSP without noble or rare elements has a wide electrochemical window and good air stability, which is very suitable for low-cost requirements in the field of grid energy storage.

Garnet-type SSEs are another class of promising electrolytes with high ionic conductivity and wide electrochemical windows. Thangadurai *et al*. [153] first prepared and characterized $Li_5La_3M_2O_{12}$ (M = Nb, Ta) with lithium-ion conductivity of 10^{-6} S cm^{-1} at room temperature. Substituting tetravalent Zr for the pentavalent position yields cubic $Li_7La_3Zr_2O_{12}$(LLZO) with ionic conductivity of 3×10^{-4} S cm^{-1}, which has drawn attention to Garnet-type SSEs [154]. While the ionic conductivity of tetragonal LLZO synthesized by Awaka *et al*. [155,156] was two orders of magnitude lower than that of the cubic phase. This change comes from the isotropic three-dimensional ion transport channel of the cubic structure, which is more conducive to the migration of Li^+. Besides crystal structure, lithium-ion conductivity in garnet-type structures is affected by lithium concentration [155] and grain boundaries [156].

The ionic conductivity of solid-state electrolytes is difficult to approach that of liquid electrolytes (10^{-3} S cm^{-1}) until a series of sulfide-based electrolytes was reported [157–159]. Kanno *et al*. [160,161] first replaced O in LISICON-type for S to obtain thio-LISICON-type SSEs, including binary Li_2S–GeS_2 and ternary Li_2S–SiS_2–P_2S_5 systems. Subsequently, it was found that $Li_{10}GeP_2S_{12}$ (LGPS) and $Li_{9.54}Si_{1.74}P_{1.44}S_{11.7}Cl_{0.3}$ had ionic conductivity comparable to or exceeding that of liquid electrolytes [162,163]. In addition to being the solid electrolyte material with the highest ionic conductivity of 2.5×10^{-2} S cm^{-1} so far, the all-solid-state cells exhibited excellent rate capabilities and cyclability (Figure 10e–g). $Li_{9.54}Si_{1.74}P_{1.44}S_{11.7}Cl_{0.3}$ has a lower cost than LGPS because of the abandonment of Ge, which is hugely exciting for aiming to replace traditional electrolytes with solid-state

electrolytes.

Halide-substituted lithium argyrodites form a new class of Li-rich solids with an unusually high Li mobility. Inspired by the similar radii of Cu^+ and Li^+, Deiseroth *et al*. [164] prepared and characterized a series of argyrodites with the general formula of Li_6PS_5X (X=Cl, Br, I). Based on molecular dynamics simulations, the origin of the Li-ion conductivity in argyrodite solid electrolytes is the presence of lithium vacancies and the distribution of the halogen ions [165]. On the one hand, the presence of halogen determines the distribution of Li vacancies. On the other hand, the disordered distribution of halide ions such as Cl^- and Br^- at multiple sites is responsible for high ionic conductivity, while I^- lacks the disorder. Furthermore, Si^{4+} replacing part of P^{5+} increased the ionic conductivity of $Li_{6+x}P_{1-x}Si_xS_5Br$ to 2×10^{-3} S cm^{-1} due to increased unit cell volume and Li^+ concentration because of larger Si [166].

Compared with crystalline solid electrolytes, the isotropic characteristics of amorphous solid electrolytes make ion channel connection easier, thus allowing the amorphous structure to obtain higher total ionic conductivity. The most well-studied glass sulfides are the binary $xLi_2S\cdot(100-x)P_2S_5$ system, where high conductivity of 1.58×10^{-3} S cm^{-1} was achieved in the solid electrolyte of $70Li_2S\cdot30P_2S_5$ [167].

Inorganic-polymer composite solid-state electrolytes. It is difficult for a single type of SSEs to meet the practical application requirements of solid-state batteries, so preparing inorganic-polymer composite materials is an expected choice. Composite SSEs inherit high ion conductivity and thermal stability of the inorganic component and the flexibility and scale-up processability of the polymer component, making them particularly suitable for the mass production of solid-state LIBs [168].

A large amount of studies around composite electrolyte design can be categorized into 'ceramic-in-polymer' and 'polymer-in-ceramic'. The ceramic-in-polymer composites have a small amount of fillers dispersed in a polymer electrolyte, designed to reduce polymer crystallinity, increase ionic conductivity, and improve mechanical properties. LLZO, a representative oxide-based electrolyte, is a widely used active inorganic filler in composite polymer electrolytes [169–171]. Nan *et al*. [172] found that the La atom of LLZO could exhibited Lewis base properties after complexing with suitable solvents, which induced the chemical dehydrofluorination of the PVDF skeleton. On this basis, a fireproof PVDF-HFP-based composite polymer electrolyte is *in-situ* synthesized with LLZO-Ga as initiator and ion-conductive filler. This *in-situ* cross-linking method avoided the influence of initiator residues on battery performance while reducing the use of organic solvents [173]. In addition to garnet-type ceramics filler, composites with various fillers and polymer hosts have also been extensively studied [174–180]. Compared with the abundant application of oxide fillers in composite polymer electrolytes, the development of sulfide/polymer composite electrolytes has encountered further obstacles due to the chemical instability of the sulfide electrolyte in diverse solvent media as well as the potential parasitic reactions between the components of the composite electrolyte [181].

The polymer-in-ceramic composites comprise compact inorganic electrolyte particles in the presence of a handful of polymers that bind particles and improve the electrode and electrolyte interface. Chen *et al*. [182] synthesized a LLZTO@PAN composite electrolyte with ultrahigh ceramic content of 94.3% *via* a solution-based precipitation process. The Lewis basicity of sulfinyl was elevated under the coupling between DMSO and LLZTO, which was responsible for the dehydrocyanation of PAN on the LLZTO surface and then the formation of the conjugated polymer coating, confirmed by TEM in Figure 6a. The conjugated structures served as continuous Li conduction pathways in the composite electrolyte, and were identified by solid-state nuclear magnetic resonance and density functional theory calculations (Figure 6b).

Tuning electrode–electrolyte interfacial stability and maintaining good interfacial contact are essential considerations in solid-state batteries. Constructing heterogeneous multilayered structures and engineering Janus interfaces are effective methods to meet the different characteristics of compatible cathodes and anodes [183–185]. Liang *et al*. [185] designed a bifunctional modified ceramic electrolyte with integrated functions of superior wettability toward electrodes and reduction resistance by fully utilizing each layer. Wang *et al*. [186] developed an *in-situ* polymerized composite electrolyte comprised of Li_6PS_5Cl and polyethylene glycol methyl ether acrylate (PEGMEA), which solved the problem of poor interfacial contact to a considerable extent confirmed by cross-sectional view and element mapping analysis. As illustrated in Figure 6c, d, the transport route priority of Li^+ in the composite electrolyte was in the order of Li_6PS_5Cl, Li_6PS_5Cl/polymer interface, and polymer.

At present, there are many kinds of inorganic electrolytes whose ionic conductivity exceeds that of liquid electrolytes in a wide temperature range [187]. Due to the immobility of the anionic framework, inorganic solid electrolytes present negligible bulk polarization. Indeed, the effects of solid electrolytes/electrode interfacial resistance are difficult to be ignored [188]. Zhang *et al*. [189] fabricated an asymmetric bilayer solid-state electrolyte by a selective adsorption and *in-situ* polymerization process. Li-based batteries with this composite electrolyte showed superior cycling stability from −20 °C–70 °C and long cycle performance at 0 °C.

4.1.2 *Electrode design for solid-state LIBs*

The design of solid-state electrodes mainly revolves around

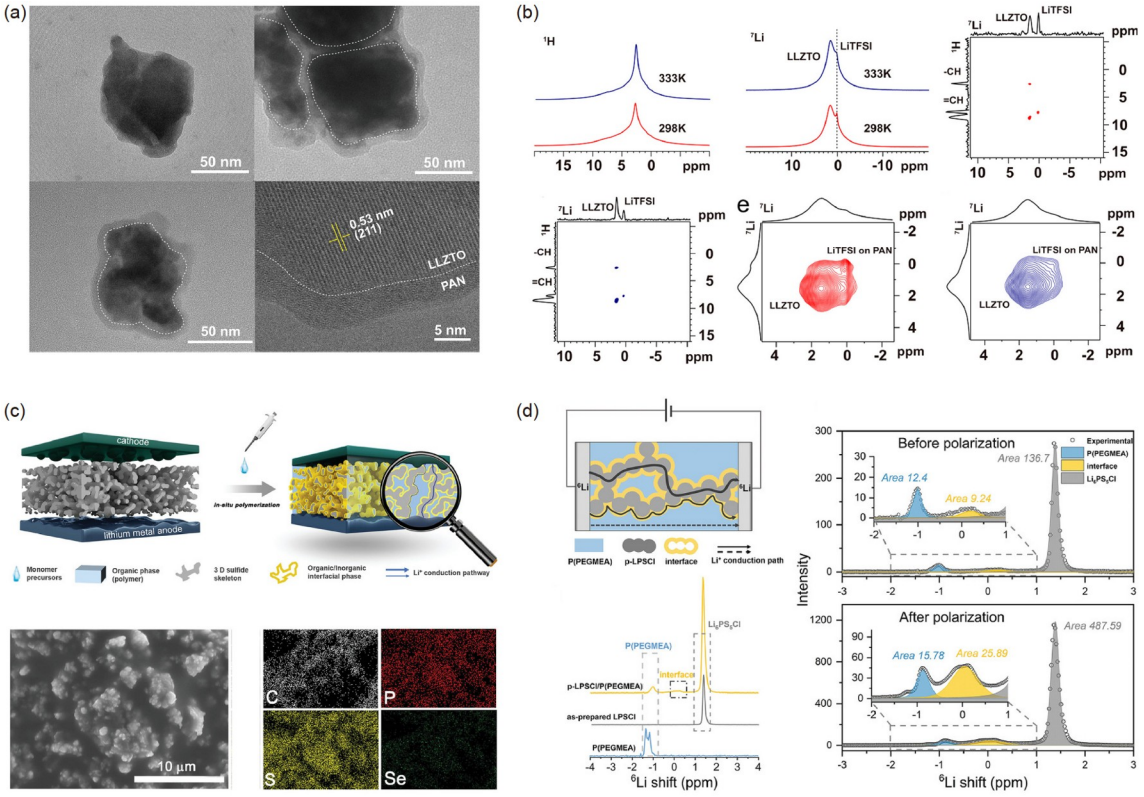

Figure 6 Advanced composite electrolytes design. (a) TEM images of LLZTO@PAN particles. (b) Solid-state MAS NMR measurements on LLZTO@PAN. Reproduced with permission from Ref. [182]. (c) Schematic illustration and cross-sectional analysis of the *in-situ* polymerization within 3D sulfide skeleton. (d) Li^+ migration behavior within the composite electrolyte. Reproduced with permission from Ref. [186] (color online).

material-level modification and electrode's structural construction, aiming to improve the compatibility of the electrode/electrolyte interface.

The high Young's modulus of the cathode-active materials (CAMs) leads to poor interface compatibility with solid-state electrolytes. Moreover, the complex composition of the cathode compartment leads to unstable chemistry, electro-chemo-mechanical breakdown, space-charge layer, *etc*. [190]. Among these problems, electrode material coating and structure design of cathodes are effective solutions.

LFP without precious metal elements has long cycle life and excellent safety performance, making it ideal for grid energy storage. Its relatively low operating voltage range and stable structure are feasible for solid electrolytes. One major obstacle is poor solid−solid contact between LFP and solid electrolyte material, which requires good adhesion by sintering the cathode and electrolyte at high temperatures. Yu *et al*. [191] performed a systematic study on the chemical stabilities between LATP and LFP at their adhesion temperatures of 500 °C–900 °C, which offered a fundamental understanding of LATP/LFP reaction mechanisms. The XRD results showed that the electrically insulating product ($Li_3Fe_2(PO_4)_3$) was responsible for the deterioration of the electrochemical performance (Figure 7a). Similarly, the extra interface layers were formed between LAGP and LFP after being sintered at 650 °C, which increased interface impedance and exacerbated the cycle [192].

Compared with LFP, the higher charging voltage of NCM makes the stability of the cathode side of the solid electrolyte face more severe challenges. Constructing a protective coating on the surface of CAMs to prevent direct contact with sulfide electrolytes is an effective strategy to improve interfacial stability [193,194]. The function of ideal CAM coatings for solid-state LIBs should involve lithium-ion transport, electron barrier, inhibition of side reactions, and buffering of CAMs strain. Although such material has not yet been found, many studies have given principles for the design of coating materials through high-throughput calculations. Several polyanionic oxides including LiH_2PO_4, $LiTi_2(PO_4)_3$, and $LiPO_3$, were highlighted for their superior performance as coating materials in solid-state LIBs [195]. Some cases demonstrate that oxide-based coatings may reduce interfacial contact impedance and improve the strength of CAMs, while detailed systematic studies are still relatively rare. More importantly, the working mechanisms behind functionalized coatings are worth further exploration [196].

To find effective methods to regulate the cathode/oxide–electrolyte interface, it is a prerequisite to clarify the mechanisms of the interfacial reaction at high temperatures.

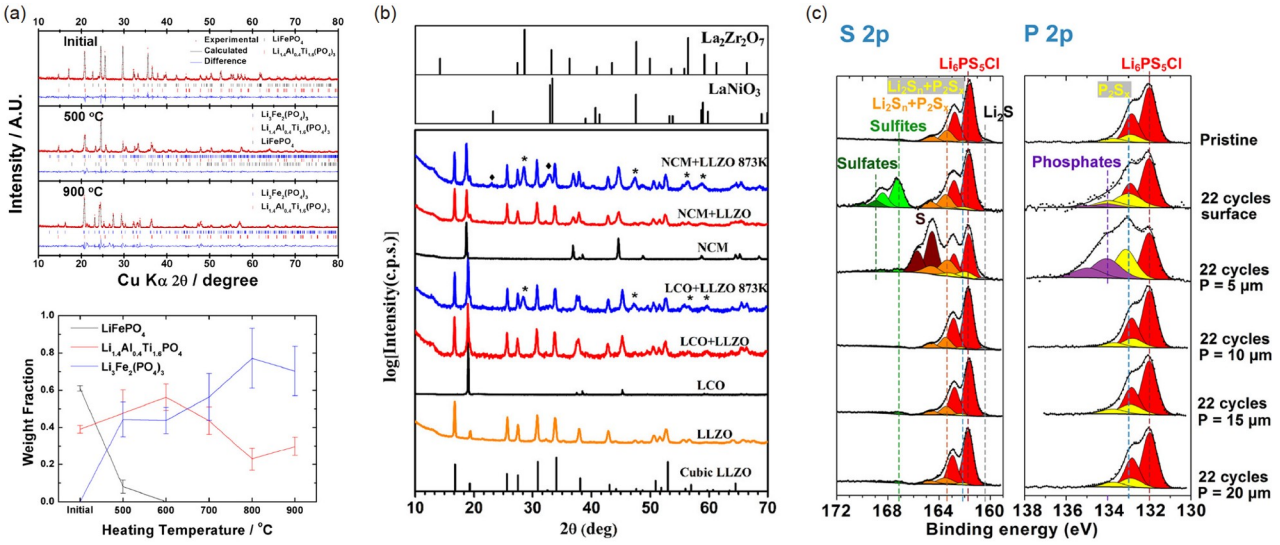

Figure 7 Interfacial parasitic products at cathode/electrolyte interfaces. (a) Chemical reactivities between LFP and LATP at various temperatures. Reproduced with permission from Ref. [191]. (b) Powder XRD patterns of the different cathodes and LLZO. Reproduced with permission from Ref. [197]. (c) XPS spectra of the composite LMO/Li_6PS_5Cl electrode. Reproduced with permission from Ref. [199] (color online).

Zhang *et al*. [197] proposed that Li, La, and Ni were sufficiently reactive to participate in diffusion at the interface. It was worth noting that Li in LLZO diffused to the Ni sites of NCM to form a Li depletion layer, which worsened the cycle performance. The peaks of pyrochlore phase ($La_2Zr_2O_7$) could be observed in co-sintered samples instead of ball-milled mixture, indicating that side reactions happen at 873 K (Figure 7b). The thermal stability of NCM is strongly affected by its composition. Fewer secondary phases appeared when Ni-rich NCM811 and LLZO were co-sintered at high temperatures [198].

The combination of CAMs and sulfide solid electrolytes faces more serious interfacial instability problems. Auvergniot *et al*. [199] observed that the greater reactivity of LMO with Li_6PS_5Cl compared to LCO and NCM could be caused by its greater potential. There is limited evidence that the oxidation products of sulfide electrolytes were detected in the pristine electrodes by XPS, implying the decomposition of electrolytes even before the beginning of the charge or discharge (Figure 7c). Exploring the ion transport path is instructive for the design of electrode structures in solid-state LIBs. Otoyama *et al*. [200] monitored the dynamic changes of ionic conduction path in the graphite anode using *operando* confocal microscopy. Introducing image analysis for rating and scoring the color changes by considering the SOC values, it was revealed that the deterioration of Li^+ ion conductivity originated from the voids and cracks (Figure 8a). And this failure was further exacerbated during charge–discharge cycling. Similar results were verified by *operando* time-of-flight secondary ion mass spectrometry (TOF-SIMS). The formation of the Li concentration gradient indicated that the charge–discharge reaction of the graphite depended on the diffusion of Li^+ within itself [201]. Although the ion transport in solid-state electrolytes is inferior to that in liquid electrolytes, the modification and optimization of the material preparation process could improve it and even achieve better rate performance than that in liquid electrolytes [202,203].

The composition of solid-state LIBs' electrodes includes active materials, conductive additives, and solid-state electrolyte, which is equivalent to the liquid electrolyte immersed in the electrode. The presence of inactive components reduces the energy density of the battery. Kim *et al*. [204] designed an electrode in which lithium-ions were accepted from the solid electrolyte interface and diffused through the electrode particles instead of the solid-state electrolyte (Figure 8b). High electronic conductivity and mechanical deformability allow graphite to independently conduct ions and electrons without electrolyte and conductive additives. The feasibility of this diffusion-dependent electrode design has been demonstrated in the practical and scalable slurry process with high loading.

The silicon-based anode is an alternative for graphite in high-energy battery systems. However, the irreversible volume deformation of silicon-based anodes in conventional LIBs leads to material fragmentation and continuous reconstruction of the SEI. Lee *et al*. [205] first reported the application of silicon anodes in glass–ceramic Li_2S–P_2S_5-based solid-state batteries. Then they optimized the particle size, conductive agent, and cut-off voltage to improve the performance of Si-containing anode in sulfide-type solid-state LIBs. Thin-film anodes once have attracted some attention [206,207], but the research interest has rapidly shifted a scalable slurry approach for preparing large-capacity

cells [208–210]. Tan *et al*. [17] enabled the stable operation of a 99.9% micro-silicon anode which removed the carbon-based conductive additive to reduce sulfide electrolyte decomposition and unwanted side reactions. Benefiting from the passive Si/sulfide electrolyte interface preventing unwanted side reactions (Figure 8c), a full pouch cell achieved a capacity of 2,800 mAh g^{-1}, and 80% capacity retention with an average CE% of >99.9% at 5 mA cm^{-2}.

The proportion of active materials in the electrodes directly determines the energy density of the fabricated cell, but many studies tend to ignore it in pursuit of performance. The inherent rigidity of oxide electrolytes brings point-to-point contact on the cathode side and increases the complexity of electron and ion transport. It is inevitable to introduce additives to improve the battery performance, which decreases active material loading and deviates from practical test conditions. For this reason, a thick cathode electrode is generally paired with polymer or sulfide electrolytes, albeit with other problems.

In addition to matching conventional electrode materials, solid electrolytes conquer enormous insurmountable difficulties occurring in liquid batteries and meet the requirements of advanced battery systems. For example, Li–S batteries with high energy densities are considered as one of the most promising energy storage devices. Some critical challenges such as Li dendrite growth, polysulfide shuttling

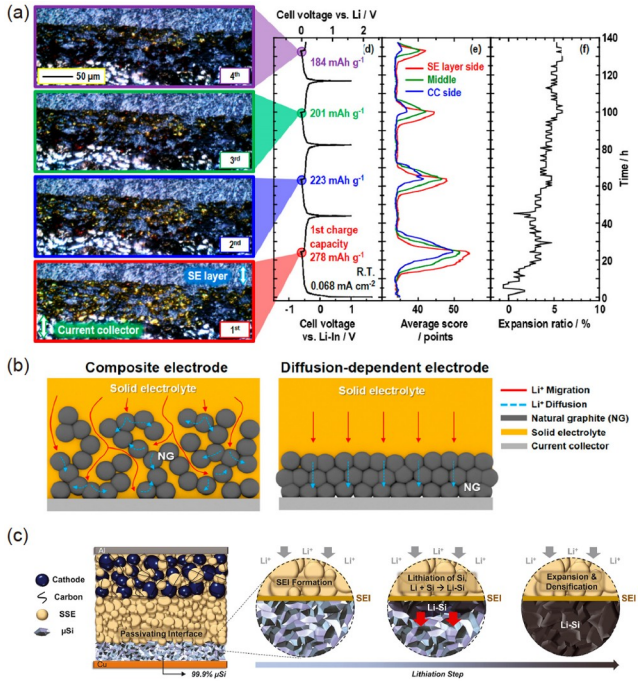

Figure 8 Collaborative design of anodes and solid-state electrolytes. (a) *Operando* confocal microscopy images of graphite electrode, corresponding charge–discharge curves, and image analysis results. Reproduced with permission from Ref. [200]. (b) Transport path of Li^+ in the composite electrode and diffusion-dependent electrode. Reproduced with permission from Ref. [204]. (c) Lithiation process of carbon-free micronsilicon anodes. Reproduced with permission from Ref. [17] (color online).

effects, unstable interfaces, are re-evaluated in solid-state batteries [211,212]. Innovative materials and battery design are expected to promote the application of solid-state Li–S batteries in energy storage systems in the future [213].

4.2 Advanced technologies for solid-state LIBs

Despite the remarkable progress achieved by researchers in the ionic conductivity of solid electrolytes, the superb performance of solid-state LIBs was still challenged by more complicated issues such as interface stability and processing method [214]. The unpredictable reactions at the electrode/electrolyte interface are attributed to complex interactions thermodynamically and kinetically. Interfacial instability under multi-field coupling is the culprit limiting cell performance. Also, the imperfection of processing methods in preparing thin and robust SSEs is the obstacle to realize low resistance and cost for practical use.

4.2.1 Stability of electrode/electrolyte interfaces

Interfacial stability issues in solid-state LIBs include chemical stability, electrochemical stability, thermal stability, and mechanical stability. We will sort out the recent progress made in interface stability, focusing on battery systems for grid energy storage.

The chemical stability of solid-state electrolytes typically refers to the compatibility with electrode materials and air sensitivity. Polymers are deemed to be chemically stable attributed to their superior compatibility with cathode/anode materials and insensitivity to water, oxygen, and carbon dioxide in the air. Therefore, a variety of polymers have been used as a protective layer for inorganic electrolyte materials [215–218]. Meanwhile, it is a caution that lithium salts in polymer electrolytes may decompose in the air.

The garnet-type LLZO, a representative of oxide electrolytes, was considered to be air-stable in previous research. However, the Li^+/H^+ exchange phenomenon widely reported in oxide-based lithium conductors resulted in the formation of a protonated LLZO phase, thus deteriorating Li^+ mobility at the interface [219]. Besides, the Li_2CO_3 generated on the surface is a decisive factor for the failure of LLZO (Figure 9a). Li_2CO_3 is partially derived from the direct reaction of LLZO and CO_2, and the remainder originated from the further reaction product of LiOH developed from LLZO and moisture in air and CO_2 [220]. As for other electrolytes in trend, perovskite-type LLTO possesses similar air stability to LLZO, while NASICON-type LATP electrolytes exhibit superior air stability and even increased ionic conductivity after brief exposure to air [221].

Sulfide electrolytes are extremely sensitive to moisture in the air and inevitably release H_2S with simultaneous structure collapse. Hard–soft acid–base (HSAB) theory is the dominant hypothesis to explain the stability of sulfide solid-

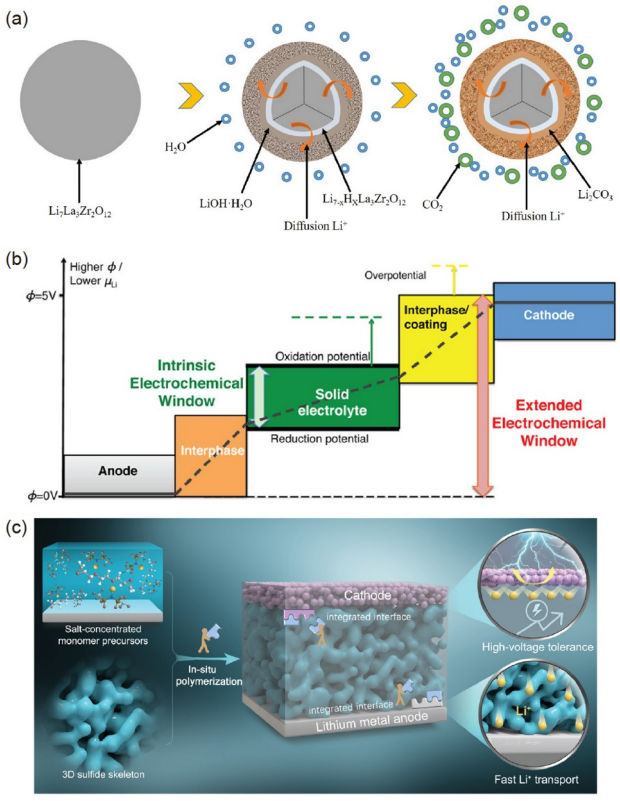

Figure 9 (a) The formation of Li_2CO_3 on the surface of LLZO. Reproduced with permission from Ref. [220]. (b) The difference between theoretical calculation and experimental results of ESWs. Reproduced with permission from Ref. [101]. (c) Integrated interface through *in-situ* polymerization. Reproduced with permission from Ref. [232] (color online).

state electrolytes in the air. Based on the empirical evidence, softer bases (S) tend to combine with soft acids such as Sn and As [222]. Zhu *et al*. [223] carried out thermodynamic analyses on the moisture stability of lithium ternary sulfides (Li–M–S) based on the first principles computation database, providing an integrated understanding of the moisture stability for sulfide solid-state electrolytes to pave the way for the development of solid-state LIBs.

Electrochemical stability is employed to evaluate the ability of materials to resist undesirable redox reactions during charge–discharge cycling. Currently, PEO-based SPEs are widely studied, but their comparatively narrow ESW (<4 V) restricts their application in high-energy density solid-state LIBs [224]. Although numerous strategies are utilized to improve the oxidation resistance of PEO, it mainly matches LFP batteries with low charging voltage now. The electrochemical stability of SPEs generally depends on the polymer matrix, lithium salt, fillers, and plasticizers. Marchiori *et al*. [225] evaluated how ESWs change when the polymers interact with the salts through density functional theory calculations. In addition, the potential catalytic effect of high-valence transition metals in cathodes on polymer electrolytes may significantly affect the interface stability, which still lacks a precise theoretical study.

Inorganic electrolytes, especially oxide-based electrolytes, generally have wider ESWs than liquid systems. Nonetheless, the impurity generated during co-sintering with cathodes is a primary cause of interfacial instability during charge–discharge cycling. The performance of solid-state battery is inevitably hindered by unexpected formation of high-resistance layers during heat treatment. Yoshinari *et al*. [226] operated and constructed a LATP-based solid-state LIB in a hot-press setup at 150 °C without high-temperature processing, which effectively suppressed the interface resistance.

Although the previous experimental results manifested that the ESWs of sulfide electrolyte cover the conventional cathode charge cut-off voltage, a narrower ESW of 1.7–2.3 V was obtained based on first-principles calculations (Figure 9b), indicating that undetected decomposition may result in the electrochemical failure [101]. Höltschi *et al*. [227] systematically investigated the effect of particle size, temperature, electrode thickness, and conductive additives on the cycling performance of graphite in sulfide solid-state LIBs. With the help of normalized cumulative irreversible charge, they proposed that the decomposition products of graphite and LPS were continuously generated throughout the cycle. Tan *et al*. [17] assembled a full cell with a nearly 100 wt% microsilicon anode, and realized over 500 cycles, because the elimination of carbon suppressed the decomposition of the LPSC at the electrode/electrolyte interface. For the cathode side, oxidative decomposition is an inevitable thermodynamic property of the sulfide electrolyte during the first cycle [228].

Thermal stability is defined as the ability of a compound to retain its original properties at elevated temperatures. The difference in the physical state between solid-state and liquid-state electrolytes determines that the former has natural advantages. The traditional PE/PP separator shrinks obviously at 150 °C, resulting in a short circuit inside the battery. The reported solid-state electrolytes can generally withstand more than 200 °C, and the decomposition temperature of oxide electrolytes even exceeds 1,000 °C. Although the formation of by-products at high temperatures may lead to the uncontrollable thermal stability of the system, it has been reported that the oxygen release from the cathode was suppressed by re-lithiation by accepting lithium-ions supplied by LLZTO [229]. Already, numerous studies qualitatively judge that solid-state LIBs possess better safety but lack more detailed quantitative characterization.

Mechanical stability refers to the capacity of a material to resist changes in stress with its original properties maintained. The parameters of its primary concern include stiffness, strength, hardness. Many efforts are devoted to improving the adaptability and tolerance of the electrolyte to the volume change of the electrode during cycling [230]. The

results of *operando* synchrotron X-ray computed microtomography elucidated that interfacial void formation and contact loss were responsible for cell failure, even for relatively soft sulfide electrolytes [231]. Jiang *et al*. [232] proposed a strategy to obtain polymer–sulfide composite electrolytes by *in-situ* polymerization, in which the polymer–sulfide composite acted as a binder to integrate the cathode and electrolyte into a coherent entity. In contrast to the composites fabricated *via ex-situ* processing, the preferable performance of the *in-situ* integrated batteries may be attributed to tight interfacial contact and reduced internal resistance, as shown in Figure 9c.

4.2.2 Processing methods

The challenges for large-scale fabrication of different types of solid electrolytes are quite different. To achieve close contact and compatible interfaces, the processing of solid-state batteries requires supplementary steps, which are rarely discussed in battery modules and packs. Next, we will focus on the optimization of the battery preparation process at different levels.

The preparation of solid-state electrolytes and the assembly of the corresponding batteries are at the heart of the whole process. The polymer electrolytes are more likely to be compatible with the roll-to-roll fabrication process applied in conventional LIBs. It's worth noting that the *in-situ* polymerization strategy could effectively fill voids between electrode particles and reduce the interface resistance, which has received considerable attention in recent years [233]. As illustrated in Figure 10a, *in-situ* polymerization could effectively fill voids between electrode particles, thus forming a continuous ion transport network.

Processing of oxide electrolytes encounters more complex challenges due to their brittle and stiff characteristics. Furthermore, the thickness of the electrolyte is inversely related to the mass and volumetric energy density of the battery. According to calculations, if the thickness of the solid electrolyte is reduced to less than 25 μm, the energy density of the pouch cell may exceed 350 Wh kg^{-1} [234]. However, the challenges associated with thin electrolyte mainly lie in the dilemma between minimizing the thickness and sustaining the mechanical strength. To date, there has been remarkable progress in developing oxide electrolytes and preparation of inorganic ceramic powder. In sharp contrast, the fabrication and optimization of thin-film oxide electrolytes was frequently overlooked. For example, the ionic conductivity of LATP powders is up to 10^{-3} S cm^{-1}, while that of the thin film is at least an order of magnitude lower [235]. In spite of the initial success in the utilization of vacuum-based techniques for fabricating thin-film batteries, the hardships in large-scale manufacturing impede their commercial implementation in grid energy storage [236–238].

Up to now, the main methods of synthesizing sulfides are melt-quenching, solution precipitation, and solid-state synthesis. Among them, solid-state synthesis, mainly ball milling, is the most widely adopted method due to its simplicity and ease of scalability. The abrasive and the sample are rolled at high speed in the grinding tank to produce strong shearing, impacting and rolling on the material to achieve the purpose of grinding (Figure 10b). The early exploration of the ball milling process was considered as a trial-and-error approach to material synthesis. Recently, Schlem *et al*. [239] detailed the basic function of ball milling and how the parameters affect the phase and structure of materials as well as the resulting battery performance.

Advanced electrode preparation processing, especially solvent-free dry-film technology, is a key step for solid-state batteries to be practical [240,241]. Meng *et al*. [242] proposed that the morphology of the binder obtained by the dry process is fibrous, which is more conducive to ion transport. Meanwhile, dry processing realizes much fewer binders and denser packing of SSE particles. A blueprint for the fabrication of solvent-free all-solid-state batteries is presented in Figure 10c.

As the research of solid-state batteries moves towards practicality and scale, reports of Ah-level solid polymer pouch cell are nothing new [243–245]. Recently, remarkable progress has been made in the preparation of inorganic solid cells, especially the sulfide-type. Since Kanno *et al*. [246] first developed all-solid-state pouch cell prototype, sheet-type solid-state pouch cells were confirmed [247,248]. Then Jung *et al*. [249] systematically investigated the electrochemical performance of conventional dry-mixed electrodes and wet-slurry fabricated electrodes. An 80×60 mm^2 $LiNi_{0.6}Co_{0.2}Mn_{0.2}O_2$/graphite full-cell exhibited a high energy density of 184 Wh kg^{-1}. Furthermore, to overcome the chemical instability of sulfide electrolytes to polar solvents, Hippauf *et al*. [250] developed a dry-film technology and verified it in pouch cell. The key indicators for evaluating the practicability of solid-state batteries are the thickness and quality of the SSE membrane. Lately, Nan *et al*. [178] fabricated a flexible LPSCl@P(VDF-TrFE) composite membrane with 30–40 μm *via* an electrospinning-infiltration-hot-pressing method. The assembled pouch-type cell presented a high capacity retention of 81% after 200 cycles at 1.0 mA cm^{-2}. With more research on practically accessible solid-state pouch cells, the commercial blueprint of solid-state batteries has gradually become clear.

Compared to batteries with liquid electrolytes, solid-state LIBs may offer a unique series (bi-polar) stacking designs without internal short-circuit issues caused by liquid electrolytes (Figure 10d). The design of bi-polar reduces the inactive current collector share of pouch cells, improving the energy density of the module and pack [251]. It is worth considering that the current collector acts as both positive

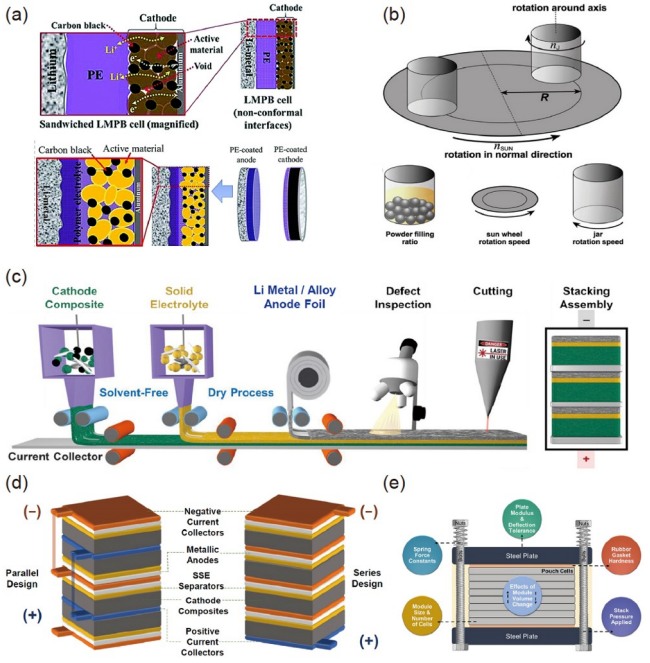

Figure 10 Fabrication of solid-state LIBs. (a) *In-situ* and *ex-situ* construction of polymer electrolytes. Reproduced with permission from Ref. [233]. (b) Schematic diagram of the planetary ball mill. Reproduced with permission from Ref. [239]. (c) Dry processing of solid-state LIBs. (d) Solid-state LIBs stack configuration. (e) Schematic of typical solid-state LIBs module assembly under stack pressure. Reproduced with permission from Ref. [242] (color online).

and negative electrodes, beyond the commonly used aluminum and copper foils.

Previous researches have substantiated that solid-state LIBs require a certain amount of pressure to operate properly. Configuring the pressure-holding device for the cell is necessary (Figure 10e), but it somehow sacrifices the energy density. Meng *et al.* [242] calculated the cell-to-module conversion efficiencies of solid-state LIBs with various stack pressures. They pointed out that the cell-to-module conversion efficiency of solid-state LIBs with the capacity over 10 kWh exceeds that of the liquid system when the applied pressure is less than 5 MPa. Additionally, the construction of the battery module, the integration of the battery pack, and the design of the built-in battery management system will be gradually perfect after the solid-state battery technologies become mature.

4.3 Safety of solid-state LIBs

In recent years, the frequent fires and explosions of traditional LIBs have seriously damaged the confidence of consumers and caused panic in the application of LIBs. Obviously, advanced solid-state electrolyte materials potentially address the limitations of commercial separators and electrolytes, while their role in battery safety still remains in vague understanding.

Compared with the analysis of intrinsic safety of electrolytes, the evaluation of solid-state LIBs is still lacking. Inoue *et al.* [252] developed an all-inclusive-microcell for differential scanning calorimetry analysis to clarify the role of each component in thermal runaway. Exothermic reactions associated with liquid electrolytes are eliminated, reducing the total heat release of solid-state LIBs to 30% of conventional LIBs. Unfortunately, solid electrolytes fail to suppress the deterioration of the electrode, such as the melting of lithium metal. Gas formation in LIBs means heat accumulation, a precursor to thermal runaway. The source of the gas mainly originated from the decomposition of SEI and the lattice oxygen release from the cathode. Torsten *et al.* [253,254] demonstrated that gas evolution caused by nickel-rich cathodes was also inevitable in thiophosphate-based solid-state LIBs. In addition to O_2, the decomposition of lithium carbonate on the cathode surface also produced CO_2, highlighting the importance of controlling impurities.

Recently, thermodynamic models were first presented to quantitatively analyze heat release from Li/LLZO/NCM111 solid-state LIBs under several failure scenarios [255]. Although solid-state LIBs show better safety when exposed to external heating, they are not necessarily safe enough in the events of internal short-circuits and mechanical failure of the SE. This distinction comes from substituting lithium metal for graphite in the high-energy-density solid-state LIBs. Additionally, a small amount of liquid electrolyte introduced into solid-state LIBs increases the total heat release, which is still significantly smaller than that of conventional LIBs.

It should be pointed out that previous research on solid-state batteries mainly revolves around lithium metal batteries, which is likely to exaggerate the safety risks of solid-state LIBs. For grid energy storage-oriented battery systems, such as LFP/graphite cells, the main risk of thermal runaway comes from unstable liquid electrolytes. Replacing all flammable and explosive organic components with thermally stable SSEs is a highly prospective solution which will significantly promote the application of LIBs in grid energy storage.

5 Summary and outlook

With the proposal of “carbon peak and neutrality” goals, optimizing the energy structure and increasing the installed capacity of renewable energy is an inevitable choice. However, the uncertainty of renewable energy supply and the stability of electric power system requirements constitute a sharp contradiction. Energy storage systems serve as a bridge to connect renewables’ generation and distribution and have the potential to address this problem. LIBs stand out from multiple types of energy storage technologies based on their superior performance. Unfortunately, the frequent safety

accidents of LIBs in recent years have irritated people's nerves. For safety and performance considerations, the iteration from traditional LIBs containing liquid electrolytes to solid-state LIBs has been in full swing. State-of-the-art solid-state LIBs exhibit high safety and excellent cycling stability, attracting widespread attention. There are still many challenges restricting their large-scale applications. The stability and safety of solid-state LIBs still need to be verified in large-capacity cells. Here are some perspectives on the application of solid-state LIBs in grid energy storage.

First, LIBs with outstanding overall performance are expected to play a predominant role in the grid energy storage market over the next several years. Understanding the degradation process and safety hazards of LIBs is critical for further optimizing LIBs' design. It is worth noting that the liquid electrolytes, composed of flammable organic solvents and thermally unstable lithium salts, are primarily responsible for the failure caused by interfacial parasitic reactions and thermal runaway. More attention should be paid to exploring intrinsically safe solid-state electrolytes to perfect the safety and cycling performance concerned by grid energy storage.

Secondly, solid-state LIBs inherit the working mechanism and preparation process of traditional LIBs, except for the upgrade of electrolytes. The characteristic of remarkable thermal stability, no volatilization, and leakage for solid-state electrolytes significantly reduce the possibility of battery thermal runaway. In addition, solid-state electrolytes offer unique cell stacking and integration of modules and packs. These advancements have accelerated the iteration of solid-state LIBs and their application in grid energy storage.

Thirdly, the research on solid-state batteries is still at the laboratory level, mainly limited by the imperfection of solid-state electrolytes. Polymer electrolytes exhibit superior stability and process compatibility, making solid-state polymer batteries close to mass production. However, introducing liquid plasticizers to boost their low ionic conductivity may cause other problems. For oxide electrolytes, large interfacial impedance caused by the inherent solid–solid point contact seriously affects the performance of solid-state LIBs. In addition, the preparation of large-capacity oxide-based solid-state LIBs still remains a thorny challenge. The rise of sulfide electrolytes has boosted confidence in the industrialization of solid-state LIBs to a certain extent. Although limitations such as narrow electrochemical windows and poor air stability still exist, its characteristics of high ionic conductivity and compatibility with scalable roll-to-roll fabrication satisfy the expectation of academia and industry. Furthermore, composite electrolyte design provides a promising strategy to balance stability, conductivity, and safety for practical solid-state LIBs.

Last but not least, interfacial stability and safety in solid-state batteries still face many challenges. In particular, the integrated design of electrolytes and electrodes needs to consider the impact of possible parasitic reactions on battery performance. The failure of the electrode/electrolyte interface during cycling is elusive due to the multi-field coupling effect. Combining theoretical calculations and advanced characterization techniques, these problems are the potential to be addressed. On the other hand, quantitative assessment of the safety of solid-state LIBs is still lacking despite the consensus on the intrinsic safety of solid-state electrolytes. Thus, more pieces of evidence need to be supplied for the safety analysis of solid-state LIBs for grid energy storage.

In summary, the remarkable superiority of solid electrolytes will drive solid-state LIBs to play a greater role in grid energy storage. The practical progress of solid-state LIBs is built on the optimization of solid-state electrolyte properties and the improvement of processing methods. Although the developing solid-state LIBs have some drawbacks, including the large interface impedance, complex processing, they will not affect the confidence of academia and industry in solid-state LIBs. It is believable that solid-state LIBs are set to have a place in future grid energy storage.

Acknowledgements This work was supported by the National Key R&D Program of China (2021YFB2400200), the CAS Project for Young Scientists in Basic Research (YSBR-058), the "Transformational Technologies for Clean Energy and Demonstration", Strategic Priority Research Program of the Chinese Academy of Sciences (XDA21070300), the National Natural Science Foundation of China (22279148, 21905286 and 22005314), the China Postdoctoral Science Foundation (2019M660805), the Special Financial Grant from the China Postdoctoral Science Foundation (2020T130658), and Beijing National Laboratory for Molecular Sciences (2019BMS20022).

Conflict of interest The authors declare no conflict of interest.

1 Sovacool BK, Ali SH, Bazilian M, Radley B, Nemery B, Okatz J, Mulvaney D. *Science*, 2020, 367: 30–33
2 Thacker S, Adshead D, Fay M, Hallegatte S, Harvey M, Meller H, O'Regan N, Rozenberg J, Watkins G, Hall JW. *Nat Sustain*, 2019, 2: 324–331
3 Kikstra JS, Vinca A, Lovat F, Boza-Kiss B, van Ruijven B, Wilson C, Rogelj J, Zakeri B, Fricko O, Riahi K. *Nat Energy*, 2021, 6: 1114–1123
4 Fuldauer LI, Thacker S, Haggis RA, Fuso-Nerini F, Nicholls RJ, Hall JW. *Nat Commun*, 2022, 13: 3579
5 van de Graaf T, Colgan J. *Palgrave Commun*, 2016, 2: 15047
6 Lebedys A, Akande D, Coent N, Elhassan N, Escamilla G, Arkhipova I, Whiteman A. Renewable capacity statistics 2022. IRENA (2022). 2022
7 Hittinger E, Whitacre JF, Apt J. *J Power Sources*, 2012, 206: 436–449
8 Yang Z, Zhang J, Kintner-Meyer MCW, Lu X, Choi D, Lemmon JP, Liu J. *Chem Rev*, 2011, 111: 3577–3613
9 Goodenough JB. *Energy Storage Mater*, 2015, 1: 158–161
10 Zhu Z, Jiang T, Ali M, Meng Y, Jin Y, Cui Y, Chen W. *Chem Rev*, 2022, 122: 16610–16751
11 Roberts BP, Sandberg C. *Proc IEEE*, 2011, 99: 1139–1144
12 Wang Q, Jiang L, Yu Y, Sun J. *Nano Energy*, 2019, 55: 93–114
13 Huang Y, Li J. *Adv Energy Mater*, 2022, 12: 2202197
14 Liu X, Cheng Y, Su Y, Ren F, Zhao J, Liang Z, Zheng B, Shi J, Zhou

K, Xiang Y, Zheng J, Wang MS, Huang J, Shao M, Yang Y. *Energy Storage Mater*, 2023, 54: 713–723
15 Jung SK, Gwon H, Lee SS, Kim H, Lee JC, Chung JG, Park SY, Aihara Y, Im D. *J Mater Chem A*, 2019, 7: 22967–22976
16 Lewis JA, Cavallaro KA, Liu Y, McDowell MT. *Joule*, 2022, 6: 1418–1430
17 Tan DHS, Chen YT, Yang H, Bao W, Sreenarayanan B, Doux JM, Li W, Lu B, Ham SY, Sayahpour B, Scharf J, Wu EA, Deysher G, Han HE, Hah HJ, Jeong H, Lee JB, Chen Z, Meng YS. *Science*, 2021, 373: 1494–1499
18 Vishnugopi BS, Hasan MT, Zhou H, Mukherjee PP. *ACS Energy Lett*, 2023, 8: 398–407
19 Luo X, Wang J, Dooner M, Clarke J. *Appl Energy*, 2015, 137: 511–536
20 Dunn B, Kamath H, Tarascon JM. *Science*, 2011, 334: 928–935
21 http://en.cnesa.org/research, accessed on 2022-08-25
22 van Noorden R. *Nature*, 2014, 507: 26–28
23 Zeng X, Li M, Abd El-Hady D, Alshitari W, Al-Bogami AS, Lu J, Amine K. *Adv Energy Mater*, 2019, 9: 1900161
24 Masias A, Marcicki J, Paxton WA. *ACS Energy Lett*, 2021, 6: 621–630
25 Li M, Lu J, Chen Z, Amine K. *Adv Mater*, 2018, 30: 1800561
26 Etacheri V, Marom R, Elazari R, Salitra G, Aurbach D. *Energy Environ Sci*, 2011, 4: 3243–3262
27 van Vliet O, Brouwer AS, Kuramochi T, van den Broek M, Faaij A. *J Power Sources*, 2011, 196: 2298–2310
28 Arteaga J, Zareipour H, Thangadurai V. *Curr Sustain Renew Energy Rep*, 2017, 4: 197–208
29 Soloveichik GL. *Annu Rev Chem Biomol Eng*, 2011, 2: 503–527
30 Hannan MA, Wali SB, Ker PJ, Rahman MSA, Mansor M, Ramachandaramurthy VK, Muttaqi KM, Mahlia TMI, Dong ZY. *J Energy Storage*, 2021, 42: 103023
31 Schmidt O, Hawkes A, Gambhir A, Staffell I. *Nat Energy*, 2017, 2: 17110
32 Li J, Fleetwood J, Hawley WB, Kays W. *Chem Rev*, 2022, 122: 903–956
33 Zhao YM, Yue FS, Li SC, Zhang Y, Tian ZR, Xu Q, Xin S, Guo YG. *InfoMat*, 2021, 3: 460–501
34 Shi JL, Xiao DD, Ge M, Yu X, Chu Y, Huang X, Zhang XD, Yin YX, Yang XQ, Guo YG, Gu L, Wan LJ. *Adv Mater*, 2018, 30: 1705575
35 Nayak PK, Erickson EM, Schipper F, Penki TR, Munichandraiah N, Adelhelm P, Sclar H, Amalraj F, Markovsky B, Aurbach D. *Adv Energy Mater*, 2018, 8: 1702397
36 Li JT, Wu ZY, Lu YQ, Zhou Y, Huang QS, Huang L, Sun SG. *Adv Energy Mater*, 2017, 7: 1701185
37 Wang YH, Li XT, Wang WP, Yan HJ, Xin S, Guo YG. *Sci China Chem*, 2020, 63: 1402–1415
38 Lu Y, Zhang Q, Chen J. *Sci China Chem*, 2019, 62: 533–548
39 Su M, Huang G, Wang S, Wang Y, Wang H. *Sci China Chem*, 2021, 64: 1131–1156
40 Zakeri B, Syri S. *Renew Sustain Energy Rev*, 2015, 42: 569–596
41 Harper G, Sommerville R, Kendrick E, Driscoll L, Slater P, Stolkin R, Walton A, Christensen P, Heidrich O, Lambert S, Abbott A, Ryder K, Gaines L, Anderson P. *Nature*, 2019, 575: 75–86
42 Shahjalal M, Roy PK, Shams T, Fly A, Chowdhury JI, Ahmed MR, Liu K. *Energy*, 2022, 241: 122881
43 Fan M, Chang X, Meng XH, Gu CF, Zhang CH, Meng Q, Wan LJ, Guo YG. *CCS Chem*, 2022, DOI: 10.31635/ccschem.022.202201996
44 Behabtu HA, Messagie M, Coosemans T, Berecibar M, Anlay Fante K, Kebede AA, Mierlo JV. *Sustainability*, 2020, 12: 10511
45 Liu J, Hu C, Kimber A, Wang Z. *J Energy Storage*, 2020, 32: 101731
46 Killer M, Farrokhseresht M, Paterakis NG. *Appl Energy*, 2020, 260: 114166
47 Argyrou MC, Christodoulides P, Kalogirou SA. *Renew Sustain Energy Rev*, 2018, 94: 804–821
48 Poullikkas A. *Renew Sustain Energy Rev*, 2013, 27: 778–788
49 Diouf B, Pode R. *Renew Energy*, 2015, 76: 375–380
50 Wu Y, Cao C. *Sci China Mater*, 2018, 61: 1517–1526
51 Hikari S. *Encyclopedia of Applied Electrochemistry*, 2014, 2165–2169
52 Zhang T, Chen Q, Li X, Liu J, Zhou W, Wang B, Zhao Z, Li W, Chao D, Zhao D. *CCS Chem*, 2022, 4: 2874–2887
53 Datta U, Kalam A, Shi J. *IEEE Trans Power Syst*, 2019, 34: 1845–1857
54 Kim J, Suharto Y, Daim TU. *J Energy Storage*, 2017, 11: 25–54
55 Gutsch M, Leker J. *J Energy Storage*, 2022, 52: 105030
56 Chen H, Cong TN, Yang W, Tan C, Li Y, Ding Y. *Prog Nat Sci*, 2009, 19: 291–312
57 Parlikar A, Truong CN, Jossen A, Hesse H. *Renew Sustain Energy Rev*, 2021, 149: 111353
58 Zubi G, Dufo-López R, Carvalho M, Pasaoglu G. *Renew Sustain Energy Rev*, 2018, 89: 292–308
59 Jaiswal A. *Renew Sustain Energy Rev*, 2017, 72: 922–934
60 Wang J, Purewal J, Liu P, Hicks-Garner J, Soukazian S, Sherman E, Sorenson A, Vu L, Tataria H, Verbrugge MW. *J Power Sources*, 2014, 269: 937–948
61 Choi D, Shamim N, Crawford A, Huang Q, Vartanian CK, Viswanathan VV, Paiss MD, Alam MJE, Reed DM, Sprenkle VL. *J Power Sources*, 2021, 511: 230419
62 Hesse H, Schimpe M, Kucevic D, Jossen A. *Energies*, 2017, 10: 2107
63 Vetter J, Novák P, Wagner MR, Veit C, Möller KC, Besenhard JO, Winter M, Wohlfahrt-Mehrens M, Vogler C, Hammouche A. *J Power Sources*, 2005, 147: 269–281
64 An SJ, Li J, Daniel C, Mohanty D, Nagpure S, Wood III DL. *Carbon*, 2016, 105: 52–76
65 Waldmann T, Hogg BI, Wohlfahrt-Mehrens M. *J Power Sources*, 2018, 384: 107–124
66 Park KJ, Hwang JY, Ryu HH, Maglia F, Kim SJ, Lamp P, Yoon CS, Sun YK. *ACS Energy Lett*, 2019, 4: 1394–1400
67 Pender JP, Jha G, Youn DH, Ziegler JM, Andoni I, Choi EJ, Heller A, Dunn BS, Weiss PS, Penner RM, Mullins CB. *ACS Nano*, 2020, 14: 1243–1295
68 Sun HH, Manthiram A. *Chem Mater*, 2017, 29: 8486–8493
69 Kubiak P, Cen Z, López CM, Belharouak I. *J Power Sources*, 2017, 372: 16–23
70 Jung SK, Gwon H, Hong J, Park KY, Seo DH, Kim H, Hyun J, Yang W, Kang K. *Adv Energy Mater*, 2014, 4: 1300787
71 Hausbrand R, Cherkashinin G, Ehrenberg H, Gröting M, Albe K, Hess C, Jaegermann W. *Mater Sci Eng-B*, 2015, 192: 3–25
72 Huang D, Engtrakul C, Nanayakkara S, Mulder DW, Han SD, Zhou M, Luo H, Tenent RC. *ACS Appl Mater Interfaces*, 2021, 13: 11930–11939
73 Zalosh R, Gandhi P, Barowy A. *J Loss Prevention Process Industries*, 2021, 72: 104560
74 Jeevarajan JA, Joshi T, Parhizi M, Rauhala T, Juarez-Robles D. *ACS Energy Lett*, 2022, 7: 2725–2733
75 Doughty DH, Roth EP. *Electrochem Soc Interface*, 2012, 21: 37
76 Mauger A, Julien CM. *Ionics*, 2017, 23: 1933–1947
77 Li H, Wang H, Xu Z, Wang K, Ge M, Gan L, Zhang Y, Tang Y, Chen S. *Small*, 2021, 17: 2103679
78 Feng X, Ren D, He X, Ouyang M. *Joule*, 2020, 4: 743–770
79 Julien C, Mauger A, Zaghib K, Groult H. *Inorganics*, 2014, 2: 132–154
80 Roth EP, Orendorff CJ. *Interface Mag*, 2012, 21: 45–49
81 Chombo PV, Laoonual Y. *J Power Sources*, 2020, 478: 228649
82 Kong L, Li C, Jiang J, Pecht M. *Energies*, 2018, 11: 2191
83 Broussely M, Biensan P, Bonhomme F, Blanchard P, Herreyre S, Nechev K, Staniewicz RJ. *J Power Sources*, 2005, 146: 90–96
84 Palacín MR. *Chem Soc Rev*, 2018, 47: 4924–4933
85 Fan E, Li L, Wang Z, Lin J, Huang Y, Yao Y, Chen R, Wu F. *Chem Rev*, 2020, 120: 7020–7063
86 Yue L, Ma J, Zhang J, Zhao J, Dong S, Liu Z, Cui G, Chen L. *Energy Storage Mater*, 2016, 5: 139–164

87 Thangadurai V, Narayanan S, Pinzaru D. *Chem Soc Rev*, 2014, 43: 4714–4727
88 Zheng F, Kotobuki M, Song S, Lai MO, Lu L. *J Power Sources*, 2018, 389: 198–213
89 Wu Y, Wang S, Li H, Chen L, Wu F. *InfoMat*, 2021, 3: 827–853
90 Li Z, Huang J, Yann Liaw B, Metzler V, Zhang J. *J Power Sources*, 2014, 254: 168–182
91 Li S, Zhang SQ, Shen L, Liu Q, Ma JB, Lv W, He YB, Yang QH. *Adv Sci*, 2020, 7: 1903088
92 Cao C, Li ZB, Wang XL, Zhao XB, Han WQ. *Front Energy Res*, 2014, 2: 25
93 Parimalam BS, MacIntosh AD, Kadam R, Lucht BL. *J Phys Chem C*, 2017, 121: 22733–22738
94 Chen R, Qu W, Guo X, Li L, Wu F. *Mater Horiz*, 2016, 3: 487–516
95 Gambe Y, Sun Y, Honma I. *Sci Rep*, 2015, 5: 1–4
96 Bruen T, Marco J. *J Power Sources*, 2016, 310: 91–101
97 Nascimento M, Novais S, Ding MS, Ferreira MS, Koch S, Passerini S, Pinto JL. *J Power Sources*, 2019, 410-411: 1–9
98 Li Y, Wang W, Yang XG, Zuo F, Liu S, Lin C. *J Power Sources*, 2022, 546: 231705
99 Zhan C, Wu T, Lu J, Amine K. *Energy Environ Sci*, 2018, 11: 243–257
100 Arora P, White RE, Doyle M. *J Electrochem Soc*, 1998, 145: 3647–3667
101 Zhu Y, He X, Mo Y. *ACS Appl Mater Interfaces*, 2015, 7: 23685–23693
102 Zhan R, Wang X, Chen Z, Seh ZW, Wang L, Sun Y. *Adv Energy Mater*, 2021, 11: 2101565
103 Lu Y, Zhao CZ, Yuan H, Hu JK, Huang JQ, Zhang Q. *Matter*, 2022, 5: 876–898
104 Cheng XB, Zhang R, Zhao CZ, Wei F, Zhang JG, Zhang Q. *Adv Sci*, 2016, 3: 1500213
105 Piątek J, Afyon S, Budnyak TM, Budnyk S, Sipponen MH, Slabon A. *Adv Energy Mater*, 2021, 11: 2003456
106 Di Lecce D, Verrelli R, Hassoun J. *Green Chem*, 2017, 19: 3442–3467
107 Chen X, Luo C, Zhang J, Kong J, Zhou T. *ACS Sustain Chem Eng*, 2015, 3: 3104–3113
108 Fan M, Meng Q, Chang X, Gu CF, Meng XH, Yin YX, Li H, Wan LJ, Guo YG. *Adv Energy Mater*, 2022, 12: 2103630
109 Chang X, Fan M, Gu CF, He WH, Meng Q, Wan LJ, Guo YG. *Angew Chem Int Ed*, 2022, 61: e202202558
110 Azhari L, Bong S, Ma X, Wang Y. *Matter*, 2020, 3: 1845–1861
111 Wang YY, Fan HH, Wang ZW, Diao WX, Fan CY, Wu XL, Zhang JP. *Chem Eur J*, 2019, 25: 15173–15181
112 Wang Y, Zhong WH. *ChemElectroChem*, 2015, 2: 22–36
113 https://www.energy.gov/, accessed on 2022-08-25
114 https://www.solidpowerbattery.com/, accessed on 2022-08-25
115 https://ses.ai/, accessed on 2022-08-25
116 https://www.quantumscape.com/, accessed on 2022-08-25
117 https://ec.europa.eu/info/index_en, accessed on 2022-08-25
118 https://www.lgensol.com/, accessed on 2022-08-25
119 https://www.samsungsdi.com/, accessed on 2022-08-25
120 https://www.toyota.ie/company/news/2021/solid-state-batteries, accessed on 2022-08-25
121 http://www.gov.cn/xinwen/2016-03/17/content_5054992.htm, accessed on 2022-08-25
122 http://www.gov.cn/xinwen/2021-03/13/content_5592681.htm, accessed on 2022-08-25
123 https://www.catl.com/, accessed on 2022-08-25
124 http://www.ganfenglithium.com/, accessed on 2022-08-25
125 https://prologium.com/, accessed on 2022-08-25
126 https://sandia.gov/ess-ssl/gesdb/public/about.html, accessed on 2023-01-08
127 https://cyprus-mail.com/2017/12/01/tesla-switches-giant-battery-shore-australias-grid/, accessed on 2023-01-08
128 http://www.prnewswire.com/news-releases/exelon-generation-and-res-announce-10-mw-battery-storage-project-300254050.html, accessed on 2023-01-08
129 http://www.speichermonitoring.de/news.html, accessed on 2023-01-08
130 https://zendure.com/, accessed on 2023-01-08
131 http://www.hydropower.org.cn/showNewsDetail.asp?nsId=31651, accessed on 2023-01-08
132 https://www.sohu.com/a/579259655_777961, accessed on 2023-01-08
133 Fenton DE, Parker JM, Wright PV. *Polymer*, 1973, 14: 589
134 Armand M. *Solid State Ion*, 1983, 9-10: 745–754
135 Zhang Y, Feng W, Zhen Y, Zhao P, Wang X, Li L. *Ionics*, 2022, 28: 2751–2758
136 Guo K, Li S, Chen G, Wang J, Wang Y, Xie X, Xue Z. *CCS Chem*, 2022, 4: 3134–3149
137 Duan H, Yin YX, Zeng XX, Li JY, Shi JL, Shi Y, Wen R, Guo YG, Wan LJ. *Energy Storage Mater*, 2018, 10: 85–91
138 Homann G, Stolz L, Neuhaus K, Winter M, Kasnatscheew J. *Adv Funct Mater*, 2020, 30: 2006289
139 Gao C, Yan D. *Prog Polym Sci*, 2004, 29: 183–275
140 Itoh T, Hirata N, Wen Z, Kubo M, Yamamoto O. *J Power Sources*, 2001, 97-98: 637–640
141 Chen Y, Shi Y, Liang Y, Dong H, Hao F, Wang A, Zhu Y, Cui X, Yao Y. *ACS Appl Energy Mater*, 2019, 2: 1608–1615
142 Su Y, Rong X, Gao A, Liu Y, Li J, Mao M, Qi X, Chai G, Zhang Q, Suo L, Gu L, Li H, Huang X, Chen L, Liu B, Hu YS. *Nat Commun*, 2022, 13: 4181
143 Tan SJ, Zeng XX, Ma Q, Wu XW, Guo YG. *Electrochem Energ Rev*, 2018, 1: 113–138
144 Mindemark J, Lacey MJ, Bowden T, Brandell D. *Prog Polym Sci*, 2018, 81: 114–143
145 Zhang J, Yang J, Dong T, Zhang M, Chai J, Dong S, Wu T, Zhou X, Cui G. *Small*, 2018, 14: 1800821
146 Chai J, Liu Z, Ma J, Wang J, Liu X, Liu H, Zhang J, Cui G, Chen L. *Adv Sci*, 2017, 4: 1600377
147 Zhou Q, Ma J, Dong S, Li X, Cui G. *Adv Mater*, 2019, 31: 1902029
148 Xu S, Sun Z, Sun C, Li F, Chen K, Zhang Z, Hou G, Cheng H-, Li F. *Adv Funct Mater*, 2020, 30: 2007172
149 Ren W, Zhang Y, Lv R, Guo S, Wu W, Liu Y, Wang J. *J Power Sources*, 2022, 542: 231773
150 Aono H, Sugimoto E, Sadaoka Y, Imanaka N, Adachi GY. *J Electrochem Soc*, 1990, 137: 1023–1027
151 Arbi K, Bucheli W, Jiménez R, Sanz J. *J Eur Ceramic Soc*, 2015, 35: 1477–1484
152 Zhu L, Wang Y, Chen J, Li W, Wang T, Wu J, Han S, Xia Y, Wu Y, Wu M, Wang F, Zheng Y, Peng L, Liu J, Chen L, Tang W. *Sci Adv*, 2022, 8: eabj7698
153 Thangadurai V, Kaack H, Weppner WJF. *J Am Ceramic Soc*, 2003, 86: 437–440
154 Murugan R, Thangadurai V, Weppner W. *Angew Chem Int Ed*, 2007, 46: 7778–7781
155 Xiang X, Chen F, Shen Q, Zhang L, Chen C. *Mater Res Express*, 2019, 6: 085546
156 Yu S, Siegel DJ. *Chem Mater*, 2017, 29: 9639–9647
157 Yang W, Tufail MK, Zhou L, Lv L, Chen R, Yang L. *Sci Sin-Chim*, 2020, 50: 1031–1044
158 Zhang Q, Cao D, Ma Y, Natan A, Aurora P, Zhu H. *Adv Mater*, 2019, 31: 1901131
159 Lee H, Oh P, Kim J, Cha H, Chae S, Lee S, Cho J. *Adv Mater*, 2019, 31: 1900376
160 Kanno R, Hata T, Kawamoto Y, Irie M. *Solid State Ion*, 2000, 130: 97–104
161 Murayama M, Kanno R, Irie M, Ito S, Hata T, Sonoyama N, Kawamoto Y. *J Solid State Chem*, 2002, 168: 140–148
162 Kamaya N, Homma K, Yamakawa Y, Hirayama M, Kanno R, Yonemura M, Kamiyama T, Kato Y, Hama S, Kawamoto K, Mitsui A. *Nat Mater*, 2011, 10: 682–686

163 Kato Y, Hori S, Saito T, Suzuki K, Hirayama M, Mitsui A, Yonemura M, Iba H, Kanno R. *Nat Energy*, 2016, 1: 16030
164 Deiseroth HJ, Kong ST, Eckert H, Vannahme J, Reiner C, Zaiß T, Schlosser M. *Angew Chem Int Ed*, 2008, 47: 755–758
165 de Klerk NJJ, Rosłoń I, Wagemaker M. *Chem Mater*, 2016, 28: 7955–7963
166 Minafra N, Culver SP, Krauskopf T, Senyshyn A, Zeier WG. *J Mater Chem A*, 2018, 6: 645–651
167 Zhang Y, Chen K, Shen Y, Lin Y, Nan CW. *Solid State Ion*, 2017, 305: 1–6
168 Fan LZ, He H, Nan CW. *Nat Rev Mater*, 2021, 6: 1003–1019
169 Bi Z, Mu S, Zhao N, Sun W, Huang W, Guo X. *Energy Storage Mater*, 2021, 35: 512–519
170 Zhao CZ, Zhang XQ, Cheng XB, Zhang R, Xu R, Chen PY, Peng HJ, Huang JQ, Zhang Q. *Proc Natl Acad Sci USA*, 2017, 114: 11069–11074
171 Xu L, Li G, Guan J, Wang L, Chen J, Zheng J. *J Energy Storage*, 2019, 24: 100767
172 Zhang X, Liu T, Zhang S, Huang X, Xu B, Lin Y, Xu B, Li L, Nan CW, Shen Y. *J Am Chem Soc*, 2017, 139: 13779–13785
173 Xu D, Su J, Jin J, Sun C, Ruan Y, Chen C, Wen Z. *Adv Energy Mater*, 2019, 9: 1900611
174 Zhai H, Xu P, Ning M, Cheng Q, Mandal J, Yang Y. *Nano Lett*, 2017, 17: 3182–3187
175 Yu X, Manthiram A. *ACS Appl Energy Mater*, 2020, 3: 2916–2924
176 Bae J, Li Y, Zhang J, Zhou X, Zhao F, Shi Y, Goodenough JB, Yu G. *Angew Chem Int Ed*, 2018, 57: 2096–2100
177 Ren Y, Cui Z, Bhargav A, He J, Manthiram A. *Adv Funct Mater*, 2022, 32: 2106680
178 Liu S, Zhou L, Han J, Wen K, Guan S, Xue C, Zhang Z, Xu B, Lin Y, Shen Y, Li L, Nan CW. *Adv Energy Mater*, 2022, 12: 2200660
179 Su Y, Zhang X, Du C, Luo Y, Chen J, Yan J, Zhu D, Geng L, Liu S, Zhao J, Li Y, Rong Z, Huang Q, Zhang L, Tang Y, Huang J. *Small*, 2022, 18: 2202069
180 Pan K, Zhang L, Qian W, Wu X, Dong K, Zhang H, Zhang S. *Adv Mater*, 2020, 32: 2000399
181 Li M, Kolek M, Frerichs JE, Sun W, Hou X, Hansen MR, Winter M, Bieker P. *ACS Sustain Chem Eng*, 2021, 9: 11314–11322
182 Chen WP, Duan H, Shi JL, Qian Y, Wan J, Zhang XD, Sheng H, Guan B, Wen R, Yin YX, Xin S, Guo YG, Wan LJ. *J Am Chem Soc*, 2021, 143: 5717–5726
183 Duan H, Fan M, Chen WP, Li JY, Wang PF, Wang WP, Shi JL, Yin YX, Wan LJ, Guo YG. *Adv Mater*, 2019, 31: 1807789
184 Duan H, Yin YX, Shi Y, Wang PF, Zhang XD, Yang CP, Shi JL, Wen R, Guo YG, Wan LJ. *J Am Chem Soc*, 2018, 140: 82–85
185 Liang JY, Zeng XX, Zhang XD, Zuo TT, Yan M, Yin YX, Shi JL, Wu XW, Guo YG, Wan LJ. *J Am Chem Soc*, 2019, 141: 9165–9169
186 Wang Y, Ju J, Dong S, Yan Y, Jiang F, Cui L, Wang Q, Han X, Cui G. *Adv Funct Mater*, 2021, 31: 2101523
187 Byeon YW, Kim H. *Electrochem*, 2021, 2: 452–471
188 Famprikis T, Canepa P, Dawson JA, Islam MS, Masquelier C. *Nat Mater*, 2019, 18: 1278–1291
189 Li J, Cai Y, Cui Y, Wu H, Da H, Yang Y, Zhang H, Zhang S. *Nano Energy*, 2022, 95: 107027
190 Judez X, Eshetu GG, Li C, Rodriguez-Martinez LM, Zhang H, Armand M. *Joule*, 2018, 2: 2208–2224
191 Yu CY, Choi J, Anandan V, Kim JH. *J Phys Chem C*, 2020, 124: 14963–14971
192 Tong H, Liu J, Qiao Y, Song X. *J Power Sources*, 2022, 521: 230964
193 Culver SP, Koerver R, Zeier WG, Janek J. *Adv Energy Mater*, 2019, 9: 1900626
194 Qi R, Shi JL, Zhang XD, Zeng XX, Yin YX, Xu J, Chen L, Fu WG, Guo YG, Wan LJ. *Sci China Chem*, 2017, 60: 1230–1235
195 Xiao Y, Miara LJ, Wang Y, Ceder G. *Joule*, 2019, 3: 1252–1275
196 Walther F, Strauss F, Wu X, Mogwitz B, Hertle J, Sann J, Rohnke M, Brezesinski T, Janek J. *Chem Mater*, 2021, 33: 2110–2125
197 Zhang N, Long X, Wang Z, Yu P, Han F, Fu J, Ren GX, Wu Y, Zheng S, Huang W, Wang C, Li H, Liu X. *ACS Appl Energy Mater*, 2018, 1: 5968–5976
198 Roitzheim C, Sohn YJ, Kuo LY, Häuschen G, Mann M, Sebold D, Finsterbusch M, Kaghazchi P, Guillon O, Fattakhova-Rohlfing D. *ACS Appl Energy Mater*, 2022, 5: 6913–6926
199 Auvergniot J, Cassel A, Ledeuil JB, Viallet V, Seznec V, Dedryvère R. *Chem Mater*, 2017, 29: 3883–3890
200 Otoyama M, Kowada H, Sakuda A, Tatsumisago M, Hayashi A. *J Phys Chem Lett*, 2020, 11: 900–904
201 Yamagishi Y, Morita H, Nomura Y, Igaki E. *J Phys Chem Lett*, 2021, 12: 4623–4627
202 Oh DY, Kim DH, Jung SH, Han JG, Choi NS, Jung YS. *J Mater Chem A*, 2017, 5: 20771–20779
203 Yang S, Yamamoto K, Mei X, Sakuda A, Uchiyama T, Watanabe T, Takami T, Hayashi A, Tatsumisago M, Uchimoto Y. *ACS Appl Energy Mater*, 2022, 5: 667–673
204 Kim JY, Park J, Lee MJ, Kang SH, Shin DO, Oh J, Kim J, Kim KM, Lee YG, Lee YM. *ACS Energy Lett*, 2020, 5: 2995–3004
205 Trevey J, Jang JS, Jung YS, Stoldt CR, Lee SH. *Electrochem Commun*, 2009, 11: 1830–1833
206 Miyazaki R, Ohta N, Ohnishi T, Sakaguchi I, Takada K. *J Power Sources*, 2014, 272: 541–545
207 Cervera RB, Suzuki N, Ohnishi T, Osada M, Mitsuishi K, Kambara T, Takada K. *Energy Environ Sci*, 2014, 7: 662–666
208 Kim DH, Lee HA, Song YB, Park JW, Lee SM, Jung YS. *J Power Sources*, 2019, 426: 143–150
209 Yamamoto M, Terauchi Y, Sakuda A, Takahashi M. *J Power Sources*, 2018, 402: 506–512
210 Dunlap NA, Kim J, Guthery H, Jiang CS, Morrissey I, Stoldt CR, Oh KH, Al-Jassim M, Lee SH. *J Electrochem Soc*, 2020, 167: 060522
211 Wu J, Liu S, Han F, Yao X, Wang C. *Adv Mater*, 2021, 33: 2000751
212 Yue J, Yan M, Yin YX, Guo YG. *Adv Funct Mater*, 2018, 28: 1707533
213 Yang X, Luo J, Sun X. *Chem Soc Rev*, 2020, 49: 2140–2195
214 Wang H, Zhu J, Su Y, Gong Z, Yang Y. *Sci China Chem*, 2021, 64: 879–898
215 Li Y, Arnold W, Thapa A, Jasinski JB, Sumanasekera G, Sunkara M, Druffel T, Wang H. *ACS Appl Mater Interfaces*, 2020, 12: 42653–42659
216 Jung WD, Jeon M, Shin SS, Kim JS, Jung HG, Kim BK, Lee JH, Chung YC, Kim H. *ACS Omega*, 2020, 5: 26015–26022
217 Jia M, Bi Z, Shi C, Zhao N, Guo X. *J Power Sources*, 2021, 486: 229363
218 Deng T, Ji X, Zhao Y, Cao L, Li S, Hwang S, Luo C, Wang P, Jia H, Fan X, Lu X, Su D, Sun X, Wang C, Zhang JG. *Adv Mater*, 2020, 32: 2000030
219 Brugge RH, Hekselman AKO, Cavallaro A, Pesci FM, Chater RJ, Kilner JA, Aguadero A. *Chem Mater*, 2018, 30: 3704–3713
220 Xia W, Xu B, Duan H, Tang X, Guo Y, Kang H, Li H, Liu H. *J Am Ceram Soc*, 2017, 100: 2832–2839
221 Dashjav E, Ma Q, Xu Q, Tsai CL, Giarola M, Mariotto G, Tietz F. *Solid State Ion*, 2018, 321: 83–90
222 Sahu G, Lin Z, Li J, Liu Z, Dudney N, Liang C. *Energy Environ Sci*, 2014, 7: 1053–1058
223 Zhu Y, Mo Y. *Angew Chem Int Ed*, 2020, 59: 17472–17476
224 Yang X, Jiang M, Gao X, Bao D, Sun Q, Holmes N, Duan H, Mukherjee S, Adair K, Zhao C, Liang J, Li W, Li J, Liu Y, Huang H, Zhang L, Lu S, Lu Q, Li R, Singh CV, Sun X. *Energy Environ Sci*, 2020, 13: 1318–1325
225 Marchiori CFN, Carvalho RP, Ebadi M, Brandell D, Araujo CM. *Chem Mater*, 2020, 32: 7237–7246
226 Yoshinari T, Koerver R, Hofmann P, Uchimoto Y, Zeier WG, Janek J. *ACS Appl Mater Interfaces*, 2019, 11: 23244–23253
227 Höltschi L, Jud F, Borca C, Huthwelker T, Villevieille C, Pelé V, Jordy C, El Kazzi M, Novák P. *J Electrochem Soc*, 2020, 167: 110558
228 Tan DHS, Wu EA, Nguyen H, Chen Z, Marple MAT, Doux JM,

Wang X, Yang H, Banerjee A, Meng YS. *ACS Energy Lett*, 2019, 4: 2418–2427
229 Wang J, Chen R, Yang L, Zan M, Chen P, Li Y, Li W, Yu H, Yu X, Huang X, Chen L, Li H. *Adv Mater*, 2022, 34: 2200655
230 He Y, Lu C, Liu S, Zheng W, Luo J. *Adv Energy Mater*, 2019, 9: 1901810
231 Lewis JA, Cortes FJQ, Liu Y, Miers JC, Verma A, Vishnugopi BS, Tippens J, Prakash D, Marchese TS, Han SY, Lee C, Shetty PP, Lee HW, Shevchenko P, De Carlo F, Saldana C, Mukherjee PP, McDowell MT. *Nat Mater*, 2021, 20: 503–510
232 Jiang F, Wang Y, Ju J, Zhou Q, Cui L, Wang J, Zhu G, Miao H, Zhou X, Cui G. *Adv Sci*, 2022, 9: 2202474
233 Vijayakumar V, Anothumakkool B, Kurungot S, Winter M, Nair JR. *Energy Environ Sci*, 2021, 14: 2708–2788
234 Balaish M, Gonzalez-Rosillo JC, Kim KJ, Zhu Y, Hood ZD, Rupp JLM. *Nat Energy*, 2021, 6: 227–239
235 Bucharsky EC, Schell KG, Hintennach A, Hoffmann MJ. *Solid State Ion*, 2015, 274: 77–82
236 Rawlence M, Filippin AN, Wäckerlin A, Lin TY, Cuervo-Reyes E, Remhof A, Battaglia C, Rupp JLM, Buecheler S. *ACS Appl Mater Interfaces*, 2018, 10: 13720–13728
237 Garbayo I, Struzik M, Bowman WJ, Pfenninger R, Stilp E, Rupp JLM. *Adv Energy Mater*, 2018, 8: 1702265
238 Kazyak E, Chen KH, Wood KN, Davis AL, Thompson T, Bielinski AR, Sanchez AJ, Wang X, Wang C, Sakamoto J, Dasgupta NP. *Chem Mater*, 2017, 29: 3785–3792
239 Schlem R, Burmeister CF, Michalowski P, Ohno S, Dewald GF, Kwade A, Zeier WG. *Adv Energy Mater*, 2021, 11: 2101022
240 Liu H, Cheng X, Chong Y, Yuan H, Huang JQ, Zhang Q. *Particuology*, 2021, 57: 56–71
241 Li Y, Wu Y, Wang Z, Xu J, Ma T, Chen L, Li H, Wu F. *Mater Today*, 2022, 55: 92–109
242 Tan DHS, Meng YS, Jang J. *Joule*, 2022, 6: 1755–1769
243 Wang Z, Shen L, Deng S, Cui P, Yao X. *Adv Mater*, 2021, 33: 2100353
244 Lu Q, Wang C, Bao D, Duan H, Zhao F, Davis KD, Zhang Q, Wang R, Zhao S, Wang J, Huang H, Sun X. *Energy Environ Mater*, 2022, DOI: 10.1002/eem2.12447
245 Wan J, Xie J, Kong X, Liu Z, Liu K, Shi F, Pei A, Chen H, Chen W, Chen J, Zhang X, Zong L, Wang J, Chen LQ, Qin J, Cui Y. *Nat Nanotechnol*, 2019, 14: 705–711
246 Inada T, Kobayashi T, Sonoyama N, Yamada A, Kondo S, Nagao M, Kanno R. *J Power Sources*, 2009, 194: 1085–1088
247 Nam YJ, Cho SJ, Oh DY, Lim JM, Kim SY, Song JH, Lee YG, Lee SY, Jung YS. *Nano Lett*, 2015, 15: 3317–3323
248 Sakuda A, Kuratani K, Yamamoto M, Takahashi M, Takeuchi T, Kobayashi H. *J Electrochem Soc*, 2017, 164: A2474–A2478
249 Nam YJ, Oh DY, Jung SH, Jung YS. *J Power Sources*, 2018, 375: 93–101
250 Hippauf F, Schumm B, Doerfler S, Althues H, Fujiki S, Shiratsuchi T, Tsujimura T, Aihara Y, Kaskel S. *Energy Storage Mater*, 2019, 21: 390–398
251 Jung KN, Shin HS, Park MS, Lee JW. *ChemElectroChem*, 2019, 6: 3842–3859
252 Inoue T, Mukai K. *ACS Appl Mater Interfaces*, 2017, 9: 1507–1515
253 Strauss F, Teo JH, Schiele A, Bartsch T, Hatsukade T, Hartmann P, Janek J, Brezesinski T. *ACS Appl Mater Interfaces*, 2020, 12: 20462–20468
254 Bartsch T, Strauss F, Hatsukade T, Schiele A, Kim AY, Hartmann P, Janek J, Brezesinski T. *ACS Energy Lett*, 2018, 3: 2539–2543
255 Bates AM, Preger Y, Torres-Castro L, Harrison KL, Harris SJ, Hewson J. *Joule*, 2022, 6: 742–755